Biochimica et Biophysica Acta 1798 (2010) 177–193

Contents lists available at ScienceDirect

Biochimica et Biophysica Acta

journal homepage: www.elsevier.com/locate/bbamem

Review

Retinal dynamics during light activation of rhodopsin revealed by solid-state NMR spectroscopy

Michael F. Brown [a,b,*], Gilmar F. J. Salgado [c], Andrey V. Struts [a,d]

[a] Department of Chemistry, University of Arizona, Tucson, AZ 85721, USA
[b] Department of Physics, University of Arizona, Tucson, AZ 85721, USA
[c] Département de Chimie, École Normale Supérieure, 75231 Paris Cedex 05, France
[d] Department of Physics, St. Petersburg State University, 198904 St. Petersburg, Russia

ARTICLE INFO

Article history:
Received 5 June 2009
Received in revised form 25 July 2009
Accepted 12 August 2009
Available online 28 August 2009

Keywords:
Molecular dynamics
G protein-coupled receptor
Membrane
Solid-state NMR
Retinal
Rhodopsin
Signal transduction
Vision

ABSTRACT

Rhodopsin is a canonical member of class A of the G protein-coupled receptors (GPCRs) that are implicated in many of the drug interventions in humans and are of great pharmaceutical interest. The molecular mechanism of rhodopsin activation remains unknown as atomistic structural information for the active metarhodopsin II state is currently lacking. Solid-state ^{2}H NMR constitutes a powerful approach to study atomic-level dynamics of membrane proteins. In the present application, we describe how information is obtained about interactions of the retinal cofactor with rhodopsin that change with light activation of the photoreceptor. The retinal methyl groups play an important role in rhodopsin function by directing conformational changes upon transition into the active state. Site-specific ^{2}H labels have been introduced into the methyl groups of retinal and solid-state ^{2}H NMR methods applied to obtain order parameters and correlation times that quantify the mobility of the cofactor in the inactive dark state, as well as the cryotrapped metarhodopsin I and metarhodopsin II states. Analysis of the angular-dependent ^{2}H NMR line shapes for selectively deuterated methyl groups of rhodopsin in aligned membranes enables determination of the average ligand conformation within the binding pocket. The relaxation data suggest that the β-ionone ring is not expelled from its hydrophobic pocket in the transition from the pre-activated metarhodopsin I to the active metarhodopsin II state. Rather, the major structural changes of the retinal cofactor occur already at the metarhodopsin I state in the activation process. The metarhodopsin I to metarhodopsin II transition involves mainly conformational changes of the protein within the membrane lipid bilayer rather than the ligand. The dynamics of the retinylidene methyl groups upon isomerization are explained by an activation mechanism involving cooperative rearrangements of extracellular loop E2 together with transmembrane helices H5 and H6. These activating movements are triggered by steric clashes of the isomerized all-*trans* retinal with the β4 strand of the E2 loop and the side chains of Glu^{122} and Trp^{265} within the binding pocket. The solid-state ^{2}H NMR data are discussed with regard to the pathway of the energy flow in the receptor activation mechanism.

Contents

Abbreviations: bR, bacteriorhodopsin; CD, circular dichroism; DARR, dipolar-assisted rotational-resonance; DOPE, 1,2-dioleoyl-*sn*-glycero-3-phosphoethanolamine; EFG, electric field gradient; ESR, electron spin resonance; FTIR, Fourier transform infrared; GPCR, G protein-coupled receptor; HOOP, hydrogen-out-of-plane; MD, molecular dynamics; meta I, metarhodopsin I; meta II, metarhodopsin II; NMR, nuclear magnetic resonance; PAS, principal axes system; PDB, Protein Data Bank; POPC, 1-palmitoyl-2-oleoyl-*sn*-glycero-3-phosphocholine; RMSD, root mean square deviation; RDC, residual dipolar coupling; RQC, residual quadrupolar coupling

* Corresponding author. Department of Chemistry, University of Arizona, Tucson, AZ 85721, USA. Tel.: +1 520 621 2163; fax: +1 520 621 8407.
E-mail address: mfbrown@u.arizona.edu (M.F. Brown).

0005-2736/$ – see front matter
doi:10.1016/j.bbamem.2009.08.013

1. Introduction

Membrane receptors, transporters, and ion channels constitute important therapeutic targets and are currently the focus of crystallographic analysis [1–14] as well as structural studies employing both solution [15–17] and solid-state [18–26] NMR spectroscopy. Yet information about the local bonding environment of cofactors is often unobtainable, and moreover knowledge of membrane protein dynamics may be difficult to acquire with either X-ray crystallography or solution NMR. In case of G protein-coupled receptors (GPCRs) such as rhodopsin, their intrinsic mobility may be functionally significant. In this article, we describe an approach using site-directed solid-state ^{2}H NMR relaxation for investigating the dynamics and interactions of the ligand in the binding pocket of the GPCR rhodopsin that reveals new information pertinent to the activation mechanism. Knowledge of the activated conformations of GPCRs as in the case of metarhodopsin II constitutes a long-sought goal, with considerable importance for biological signaling mechanisms and pharmaceutical design. More generally, a flow of energy is involved in activating movements of membrane proteins, whose conformational transitions occur on a multidimensional energy landscape [27–29].

To understand the activation of rhodopsin, one must characterize the atomistic motions of the ligand and the protein as well as establish the role of the membrane lipid bilayer. Photon absorption by the retinal ligand yields helical movements of rhodopsin [30] that result in activation of the photoreceptor through exposure of recognition sites on the cytoplasmic loops for the G protein (transducin). Such helical movements are triggered by changes in the retinylidene conformation due to isomerization, followed by rearrangement of hydrogen-bonding networks around Glu^{122} [31] and the extracellular E2 loop [26], deprotonation of the retinylidene Schiff base, and disruption of two ionic locks stabilizing the dark state conformation [32–34]. An allosteric network couples the retinal cofactor to rhodopsin [35], which in turn is coupled to the membrane lipid bilayer [36,37]. The free energy of the bound ligand provided by photon absorption elicits a conformational change of the protein that leads to the biological response [37]. Visual signaling results through the action of effector proteins [38] in two amplification stages, involving sequential activation of the G protein transducin followed by stimulation of a cGMP phosphodiesterase. Closing of GMP-gated cation-selective channels in the rod plasma membrane leads to membrane hyperpolarization and the generation of a visual nerve impulse.

At the molecular level, X-ray crystal structures are available for the rhodopsin [1–5], bathorhodopsin, and lumirhodopsin states [6], and a low-resolution structure of a photoactivated deprotonated intermediate [7]. Recent structures for the ligand-free opsin [39] and the transducin-activating conformation with a bound peptide [40] may retain structural elements of the activated meta II state. The latter studies [39,40] strikingly corroborate earlier site-directed spin-labeling studies [41] that reveal helical movements coupled to light-induced conformation changes of rhodopsin due to 11-*cis* to *trans* isomerization of the retinylidene cofactor [42,43]. In addition, plasmon waveguide resonance spectroscopy [44,45] shows a light-induced elongation of the protein that occurs following light absorption, as experimentally visualized in the X-ray crystal structure of the ligand-free opsin apoprotein [39]. Within this context, solid-state NMR spectroscopy is complementary to X-ray crystallography and other spectroscopic methods [46–48]. First, one can obtain structural information that in some respects may be more accurate than X-ray studies. Second, membrane proteins are studied in a native-like membrane environment [20,21,25,49–54], where protein function is preserved [37,55]. Last, solid-state NMR relaxation experiments reveal dynamical knowledge for non-crystalline biomembrane specimens that cannot be obtained with X-ray or other methods [56]. It is mainly theoretical molecular dynamics (MD) simulations that provide such comprehensive dynamical information at present [33], which require validation through experimental studies as described here. The results of solid-state ^{2}H NMR spectroscopy thus provide an avenue or input into the structural dynamics that can be particularly useful in combination with all-atom MD simulations [57,58].

Studies of rhodopsin mutants have been instrumental in identifying key interactions that may not always be evident from the X-ray structure [32,38]. Moreover, biophysical and bioorganic studies of rhodopsin regenerated with various retinal analogues have identified the parts of the cofactor that are implicated in biological activity [59]. The methyl groups of retinal lead to conformational distortion that is linked to the biological function of rhodopsin [35,46]. The C5-, C9-, and C13-methyl groups each occupy distinct protein binding sites for the chromophore; the β-ionone ring with the C5-methyl is in a hydrophobic pocket; the polyene chain with its C9-methyl group is situated in a slot between the side chains of Thr^{118} on helix H3 and Tyr^{268} on H6; and the C13-methyl group is located between the 11-*cis* double bond and the protonated Schiff base with its associated counterion. The retinylidene methyl groups are known to be important for the photochemistry and activation of rhodopsin [31,35]. For example, studies of 5-desmethyl analogs show that deletion of the C5-methyl has a dramatic effect on rhodopsin regeneration and the transition from meta I to meta II [31]. Indications that the C5-methyl group is involved in interaction with Glu^{122} have been found in an FTIR study of desmethyl analogs of retinal bound to rhodopsin [31], which is also supported by close proximity of the C5-methyl group to Glu^{122} in the crystal structure [4]. Moreover, the β-ionone ring of the retinylidene ligand may be implicated in the spectral properties [60] and activation of rhodopsin [31,59,61–64]. The ring moiety of retinal may function through maintaining the activated meta II conformation of rhodopsin [31,64,65]. Acyclic analogs of retinal lacking the β-ionone ring act as partial agonists, as they shift the metarhodopsin equilibrium toward the inactive meta I state [31,61]. Removal of the C9-methyl group leads to a relaxation of

chromophore strain [66] giving a partial agonist [35,46,64], which shifts the meta I to meta II equilibrium toward the inactive meta I state, with diminished transducin activation [64]. Absence of the C9-methyl group also perturbs the positioning of the ring of retinal in its binding site, leading to an altered hydrogen bonding of Glu^{122} [35]. Finally, deletion of the C13-methyl group gives less intense hydrogen-out-of-plane (HOOP) modes in vibrational spectroscopy [35,67], together with a decreased photoreaction rate and quantum yield [68]. Deletion of the C13-methyl group also shifts the metarhodopsin equilibrium toward the inactive meta I state [35].

Experimental data on rhodopsin structure and dynamics in the intermediates and the active state are very limited at present, and mainly come from Raman [47] and FTIR [69] spectroscopy, spin-label ESR [43,70], solid-state NMR [24–26,71–74], and MD simulations [57,58,75,76]. Vibrational spectroscopy reveals HOOP modes of the retinal chromophore, which provide information about its torsional twisting. It is mainly in the case of NMR that one can obtain both structural and dynamical information over picosecond–nanosecond time scales. Yet the full potential of solid-state NMR in studies of biomembranes has not been explored to date, as a combined approach involving both NMR spectral line shapes and relaxation methods has not been extensively implemented for membrane proteins such as rhodopsin. In this article, we review the application of solid-state ^{2}H NMR to rhodopsin and show that combined line shape and relaxation methods can play a key role in establishing the ligand conformation within the binding cavity, and the changes that occur in the receptor activation.

2. Solid-state NMR spectroscopy is a powerful tool in membrane biophysics

Investigations of molecular solids, liquid crystals, membranes, and protein aggregates are all possible with solid-state NMR [77]. In particular, site-directed ^{2}H NMR is a valuable tool to study the local structure and dynamics of biomolecules under conditions preventing isotropic molecular motion. By contrast, in solution NMR one cannot readily analyze various types of local motions, and separation of different motions takes place only on a time-scale basis [78–80]. Protein rotational diffusion is typically detected in solution NMR relaxation studies, so that further analysis is needed to extract the internal structural and dynamical information [78–80]. The general reader should recognize that in solid-state NMR spectroscopy we do not necessarily observe actual solid samples. Rather, one studies the anisotropy of the magnetic or electrical interactions that are incompletely averaged away by the molecular fluctuations. Even in the presence of considerable molecular motion, it is possible for residual anisotropies to exist, as in the case of liquid crystals [81–83]. As a result, the magnetic or electrical interactions in NMR spectroscopy provide a rich source of information about structure and dynamics for membrane proteins 21,84–94] and peptides [95–103], lipid bilayers [104–108], biopolymer fibers [109,110], amyloid fibrils [111–118], and inclusion bodies [119].

2.1. Structure, dynamics, and orientations of membrane-bound peptides and proteins are revealed by solid-state NMR

In the context of structural biology, ^{2}H NMR spectroscopy constitutes a useful approach for probing the structure and dynamics of integral membrane proteins in a native-like membrane environment. Solid-state ^{2}H NMR [91] is complementary to solid-state ^{13}C NMR [22,26,73,120] in that orientational restraints are provided [24], which together with distance restraints [22,73] allow site-specific structural information to be obtained analogous to solution NMR [121,122]. In solid-state ^{2}H NMR of biomembranes, the motionally averaged spectral line shapes involve residual quadrupolar couplings (RQCs) that correspond directly to the segmental order parameters [83,123]. The RQCs can be measured directly together with the corresponding dynamical parameters, viz nuclear spin relaxation rates such as the relaxation of Zeeman order (R_{1Z}) or quadrupolar order (R_{1Q}). By contrast, in X-ray structures the mobility enters through the Debye–Waller factors that do not distinguish static from dynamic disorder [124]. It naturally follows that NMR is ideal for observing both structure and dynamics of solid-like or liquid-crystalline samples, which can have considerable internal mobility, or liquid-like samples that conversely can have a local structure.

2.2. Rhodopsin is a G protein-coupled receptor that can be studied by NMR spectroscopy

Because NMR detects both structure and dynamics, it provides input to the overarching questions in the fields of rhodopsin and GPCRs in cellular membranes [125]. These include (*i*) understanding how retinal can be so unusually stable in the dark state, yet become instantly transformed upon light absorption, as well as (*ii*) establishing how the light-induced changes are propagated from the retinal binding pocket through an allosteric network within the protein to the cytoplasmic loops that contain the activation sites for recognition of the G protein (transducin). Conformational strain of retinal has long been postulated to play a major role in the remarkable photochemistry of rhodopsin, as shown by vibrational [47], linear dichroism [126], and solid-state NMR [22,52,73] spectroscopy as well as MD simulations [76]. Upon light absorption the switch is virtually instantaneous and 11-*cis* to *trans* isomerization occurs within only 200 fs [47]. Yet the retinal ligand is phenomenally stable in the dark state, with a spontaneous rate of isomerization estimated to occur only once in several millennia [127]. Activating movements of the protein are triggered by the ligand involving an energy landscape whereby the roughness depends on the length scale. Over relatively short distances, thermal fluctuations of the ligand occur within a given state at relatively high frequencies, whereas over larger distances matching of the ligand to protein fluctuations at lower frequencies can drive conformational transitions producing the biological response.

Solid-state NMR has been extensively applied to investigations of rhodopsin including magic-angle spinning ^{13}C NMR [25,26,65,128–130], ^{15}N NMR [131], and ^{2}H NMR [24,52,53,56,132]. Both the protein as well as the bound retinal ligand have been investigated with solid-state ^{13}C NMR of rhodopsin in detergent micelles [25,26,130]. Complementary ^{2}H NMR studies of the retinal cofactor of rhodopsin in a native-like membrane environment have also been conducted [24,52,53,56,132]. The ^{2}H NMR structure of 11-*cis*-retinal in the dark state reveals dihedral twisting of the polyene chain and the β-ionone ring, in contrast to microbial rhodopsins such as bacteriorhodopsin. Analysis of the angular-dependent ^{2}H NMR line shapes of selectively deuterated methyl groups in rhodopsin in aligned membranes allows accurate determination of the equilibrium ligand conformation in the binding pocket [24]. For rhodopsin, the retinal cofactor is locked within the binding pocket with a negative pre-twist about the C11═C12 double bond, which explains its dark state stability as well as its rapid photochemistry, and also indicates the trajectory of the light-induced 11-*cis* to *trans* isomerization [24]. According to ^{2}H NMR, the retinal strain is progressively relaxed in forming the pre-activated meta I state. Additional relaxation studies allow one to obtain dynamical information about the dark and pre-activated meta I state as well as the activated meta II state. In this respect, knowledge of the mobility of retinal bound to rhodopsin may help to understand the functional dynamics of the ligand in relation to the activation mechanism.

3. Analysis of solid-state ^{2}H NMR line shapes gives residual quadrupolar couplings and orientations for methyl groups of retinal bound to rhodopsin

Here we applied site-directed ^{2}H NMR spectroscopy to study the retinal cofactor structure and dynamics within the binding pocket of

rhodopsin in the dark state as well as the pre-activated meta I and active meta II intermediates. Rhodopsin has been investigated in planar-supported membranes as a function of the tilt angle to the magnetic field under conditions where rotational and translational diffusion of the protein on the ^{2}H NMR time scale are effectively quenched [24]. The oriented membranes involve substantial alignment disorder, and thus a proper treatment of the mosaic spread is pivotal to determining accurate bond orientational restraints [133]. One of the important features of NMR spectroscopy is that information about mobility can be obtained directly from the NMR line shape. For example, residual dipolar and quadrupolar couplings (RDCs and RQCs, respectively) in NMR spectra provide information about order parameters related to the mean orientation of the nuclear interaction tensor as well as dynamical disorder. In addition, the intrinsic line broadening is proportional to the transverse (R_2) relaxation rate, which in turn is related to molecular mobility, whereby narrower NMR lines correspond to faster motion. Further detailed information about dynamics is obtained from longitudinal (R_{1Z}) and quadrupolar order (R_{1Q}) relaxation experiments, as described subsequently.

3.1. Powder-type ^{2}H NMR spectra indicate rapid rotation of methyl groups with restricted off-axial fluctuations

Residual quadrupolar couplings have been obtained from the powder-type NMR spectra of rhodopsin containing retinal labeled with ^{2}H at the C5-, C9-, or C13-methyl groups in POPC recombinant membranes. For random (powder type) membrane dispersions, the ^{2}H NMR line shapes correspond to a Pake doublet [81,134]. The RQCs for the C5-, C9-, and C13-methyl groups indicate that they all undergo fast spinning about their C_3 axes with correlation times $<10^{-5}$ s (motional narrowing) with restricted off-axial fluctuations. The order parameter of the methyl group characterizes the amplitude of the fluctuations of retinal within the binding pocket of rhodopsin and is given by $S_{C_3} \equiv (1/2)\langle 3\cos^2\beta_{MD} - 1\rangle$, where β_{MD} is the angle between the instantaneous and average methyl group orientation. Comparison of the value of the residual (motionally averaged) quadrupolar coupling $\langle\chi_Q\rangle$ with the value of χ_Q corresponding to the rotation of methyl group yields $S_{C_3} \approx 0.9$, which corresponds to an amplitude of the off-axial fluctuations of $\beta_{MD} \approx 15°$. This motion includes libration of the methyl groups with respect to the unsaturated polyene as well as any reorientations of the polyene chain and β-ionone ring within the binding pocket. Little variation of the intrinsic line broadening and derived T_2 relaxation times was observed within the temperature interval from −150 to −30 °C. In conjunction with relaxation time measurements (see below), we also obtain knowledge of the associated correlation times.

3.2. Solid-state ^{2}H NMR line shapes for retinal cofactor of rhodopsin in aligned membranes provide average methyl orientations

Theoretical ^{2}H NMR spectra for the oriented samples can be calculated by assuming a static uniaxial distribution about the average membrane normal [133]. The theoretical line shapes depend on both the methyl bond orientation θ_B with respect to the membrane normal (Fig. 1) as well as the alignment disorder (mosaic spread), which is assumed to be Gaussian with a standard deviation of σ. In gel-state bilayers, membrane proteins do not undergo significant rotational diffusion [135] on the ^{2}H NMR time scale ($\approx$10 μs). The quadrupolar frequencies of the two spectral branches can be expressed as [134]

$$\nu_Q^{\pm} = \pm \frac{3}{4}\chi D_{00}^{(2)}(\Omega_{XL}). \quad (1)$$

where χ is the coupling constant (static $\chi = \chi_Q = 170$ kHz; or residual $\chi = \langle\chi_Q\rangle$); the symbol $\mathbf{D}^{(j)}$ designates the Wigner rotation matrix of rank j, and $\Omega_{XL} = (\tilde{\phi}, \tilde{\theta}, 0)$ are the Euler angles which

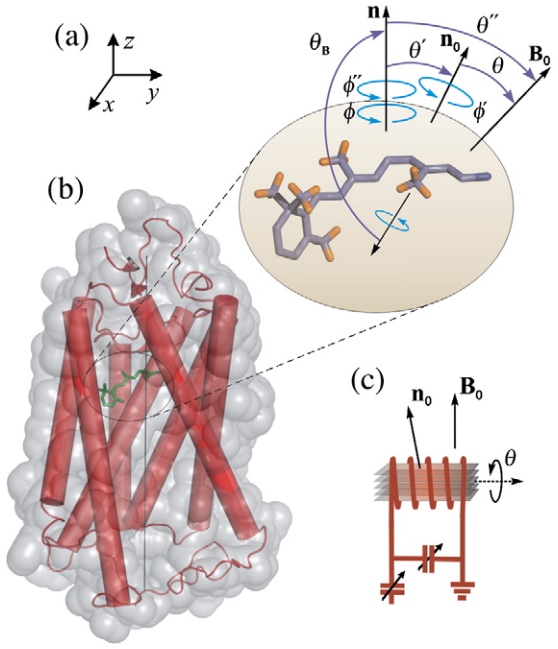

Fig. 1. Structure and dynamics of retinal ligand of rhodopsin are probed by solid-state ^{2}H NMR spectroscopy in a native-like membrane environment. Geometry of the NMR experiment is depicted for aligned bilayers. (a) 11-*cis*-retinylidene chromophore of rhodopsin in the dark state. Angle of C–C^{2}H$_3$ bond axis to the local membrane normal **n** is designated as θ_B, with static rotational symmetry described by azimuthal angle ϕ. Alignment disorder is characterized by angle θ' of **n** relative to the average membrane normal $\mathbf{n_0}$ and is uniaxially distributed as given by Φ'. The tilt angle of $\mathbf{n_0}$ to the main magnetic field $\mathbf{B_0}$ is denoted by θ about which there is also cylindrical symmetry. Finally, θ'' and ϕ'' are the angles for overall transformation from **n** to $\mathbf{B_0}$. (b) Membrane-bound rhodopsin including the *N*-retinylidene cofactor within its binding cavity. The van der Waals surface of rhodopsin is depicted in light grey, with the seven transmembrane helices indicated by rods. Note that the extracellular side is at top and the cytoplasmic side at bottom. (c) Schematic view of stack of aligned membranes containing rhodopsin within the radiofrequency coil of the NMR spectrometer, showing geometry relative to the $\mathbf{B_0}$ magnetic field. Adapted with permission from Ref. [24].

transform the irreducible components of the coupling tensor from its principal axes system (PAS; molecule fixed) to the laboratory coordinate frame, defined by the main magnetic field $\mathbf{B_0}$. An axially symmetric coupling tensor, i.e., $\eta = 0$, is assumed. For a rotating methyl group, the static coupling constant is averaged to $\chi_Q^{eff} = \chi_Q\ (3\cos^2 109.47° - 1)/2 = (-1/3)\ \chi_Q = -56.67$ kHz. Off-axial fluctuations are characterized by $S_{C_3} = \langle\chi_Q\rangle / \chi_Q^{eff}$, which is the order parameter of the methyl three-fold (C_3) axis, where the brackets denote a time average.

The solid-state ^{2}H NMR spectrum is described by the distribution of the spectral intensity as function of frequency, which can be represented in terms of the reduced frequencies $\xi_\pm$ for each of the spin $I = 1$ spectral branches. For an axially symmetric coupling tensor $\xi_\pm \equiv \nu_Q^{\pm}/(3/4)\chi$, that is to say, $\xi_\pm = \pm D_{00}^{(2)}(\tilde{\theta}) = (\pm 1/2)(3\cos^2\tilde{\theta} - 1) \in [\mp 1/2,\ \pm 1]$ [134]. Moreover, the elements of the Wigner rotation matrix transform according to [134]

$$D_{00}^{(j)}(\Omega_{XL}) = \sum_{m'=-2}^{2} \sum_{m=-2}^{2} D_{0m'}^{(j)}(\Omega_{XN}) D_{m'm}^{(j)}(\Omega_{ND}) D_{m0}^{(j)}(\Omega_{DL}). \quad (2)$$

The first Euler angles $\Omega_{XN} \equiv (0, \theta_B, \phi)$ include the orientation of the PAS of the coupling tensor ($X \equiv$ static or residual) relative to the local membrane normal **n**, where θ_B is the bond orientation (N frame) and ϕ is the random azimuthal rotation about the local normal (cf. Fig. 1). The second set $\Omega_{ND} \equiv (0, \theta', \phi')$ treats the disorder of the local membrane normal relative to the average normal $\mathbf{n_0}$ to the membrane surface (D frame) in terms of θ' as well as the random azimuth ϕ'. The final transformation describes the inclination (tilt) of the average membrane normal to the laboratory (L) frame (static magnetic field

$\mathbf{B_0}$). The analytical calculation can be simplified by introducing rank-1 rotation matrix elements [133], giving

$$\cos\tilde{\theta} = \cos\theta_B\cos\theta'' - \sin\theta_B\sin\theta''\cos(\phi+\phi'') \quad (3)$$

$$\cos\theta'' = \cos\theta'\cos\theta - \sin\theta'\sin\theta\cos\phi' \quad (4)$$

Here the extra angles $\Omega_{NL}\equiv(\phi'',\theta'',0)$ describe the overall rotation of the local frame to the laboratory, where θ'' is the tilt of the local normal and ϕ'' is a phase factor that connects the two transformations [133].

The following formulas are obtained for the line shape representing the two $I=1$ spectral branches of the ^{2}H nucleus [133]:

(*i*) if $\alpha>\gamma>\delta>\beta$ or $\gamma>\alpha>\beta>\delta$, then

$$|p(\xi_{\pm})| \propto \frac{1}{|\cos\tilde{\theta}|}\int_0^{\pi}\frac{1}{y}K\left(\frac{x}{y}\right)\exp\left(\frac{-\theta'^2}{2\sigma^2}\right)\sin\theta'\,d\theta' \quad (5)$$

(*ii*) if $\gamma>\alpha>\delta>\beta$ or $\alpha>\gamma>\beta>\delta$, then

$$|p(\xi_{\pm})| \propto \frac{1}{|\cos\tilde{\theta}|}\int_0^{\pi}\frac{1}{x}K\left(\frac{y}{x}\right)\exp\left(\frac{-\theta'^2}{2\sigma^2}\right)\sin\theta'\,d\theta' \quad (6)$$

Here $x\equiv\sqrt{(\gamma-\delta)(\alpha-\beta)}$ and $y\equiv\sqrt{(\alpha-\delta)(\gamma-\beta)}$, and the cosines of the sum and difference angles are defined as follows: $\alpha\equiv\cos(\tilde{\theta}-\theta_B)$; $\beta\equiv\cos(\tilde{\theta}+\theta_B)$; $\gamma\equiv\cos(\theta-\theta')$; and $\delta\equiv\cos(\theta+\theta')$). The kernel $K(k)=F(\pi/2,k)$ constitutes a compete elliptic internal of the first kind in the normal trigonometric form:

$$K(k) = \int_0^{\pi/2}\frac{dx}{\sqrt{1-k^2\sin^2 x}} \quad (7)$$

The 3-D alignment disorder (mosaic spread) is described by a Gaussian distribution of the local membrane normal versus the average bilayer normal, $P(\theta') = \left(1/\sigma\sqrt{2\pi}\right)\exp(-\theta'^2/2\sigma^2)$, where σ is the standard deviation about the mean of $\langle\theta'\rangle=0$. For a random (spherical) distribution, the line shape formula gives the well-known Pake doublet:

$$|p(\xi_{\pm})| \propto \frac{1}{|\cos\tilde{\theta}|} \propto \frac{1}{\sqrt{1\pm 2\xi_{\pm}}} \quad (8)$$

4. Structural analysis of retinal in the dark and meta I states shows torsional twisting and deformation of the bound cofactor

By aligning the POPC membranes containing rhodopsin on planar substrates, one can determine the orientation of the ^{2}H quadrupolar coupling tensor relative to the membrane frame. Simulations of experimental ^{2}H NMR spectra employed the above line shape formulas, Eqs. (5)–(7) for a static uniaxial distribution [133], as also applied previously to bacteriorhodopsin (bR) in purple membranes [50] and to aligned DNA fibers [109]. For oriented samples, the simulation parameters include the C–C^{2}H$_3$ bond orientation, the mosaic spread, the residual coupling $\langle\chi_Q\rangle$, and the intrinsic line broadening. Alternatively, a Monte Carlo simulation of the line shapes was also introduced to cross-validate the above procedure. The line shape was accumulated numerically by randomly generating the angular variables according to their distribution functions, as in Eqs. (1)–(4), together with the Gaussian distribution for the mosaic spread [133], giving essentially identical results to the closed-form analysis. The degree of membrane orientation was also investigated by ^{31}P NMR spectroscopy. Compared to previously published data [136], complete membrane alignment was not obtained, but rather aligned fractions of ≈90% were typical for rhodopsin in POPC or DMPC bilayers. In the case of unoriented (powder-type) samples, the Pake formula, Eq. (8), is used. The current findings can be summarized as follows. (*i*) In the dark state, the binding pocket induces a pre-twisting of the 11-*cis*-retinal around the C11=C12 double bond, which results in the fast and efficient isomerization of the ligand. (*ii*) In the meta I state, the β-ionone ring is displaced by about 1 Å toward helices H3 and H5 whereas the part of the polyene chain between the C9-methyl group and protonated Schiff base moves toward Trp^{265}. The implications of these structural changes on the activation mechanism are further discussed below.

4.1. Solid-state ^{2}H NMR structure of retinal in the dark state assumes three planes of unsaturation

Referring to Fig. 1, the experimental arrangement involves a stack of supported membranes containing rhodopsin labeled at the C5-, C9-, or C13-methyl groups. Rhodopsin is depicted by the seven transmembrane helices within the van der Waals surface of the receptor. The retinylidene ligand is shown at top right to illustrate the structure determination. The orientation θ_B of the C–C^{2}H$_3$ bond

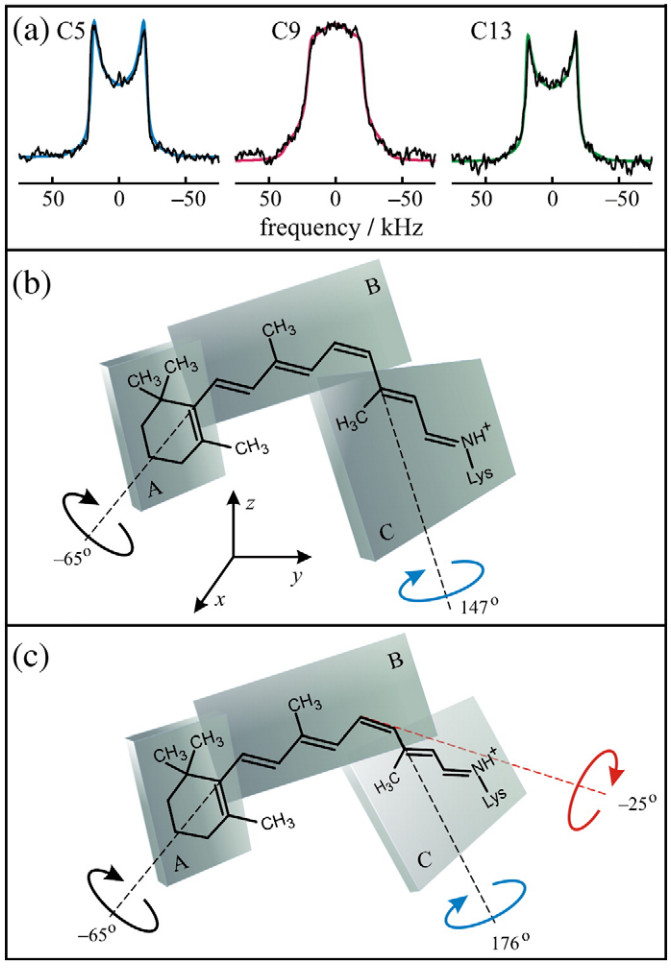

Fig. 2. Solid-state ^{2}H NMR allows determination of structure and orientation of 11-*cis*-retinal in the dark state of rhodopsin. The retinal conformation is described by three planes of unsaturation (designated A, B, C). (a) ^{2}H NMR spectra for 11-*cis*-retinal in the rhodopsin dark state depend on the methyl bond orientation and mosaic spread of aligned membranes. Representative ^{2}H NMR spectra are shown for 11-*Z*-[5-C^{2}H$_3$]-retinylidene rhodopsin (blue), 11-*Z*-[9-C^{2}H$_3$]-retinylidene rhodopsin (magenta), and 11-*Z*-[13-C^{2}H$_3$]-retinylidene rhodopsin (green), respectively. Results are included for rhodopsin/POPC bilayers (1:50) at $\theta=0°$ orientation of membrane normal to the static magnetic field $\mathbf{B}_0$ at pH = 7 and $T=-150$ °C. (b) Simple three-plane model having dihedral twisting only about C6–C7 and C12–C13 bonds. (c) Extended three-plane model with additional pre-twisting about C11=C12 double bond. Note that the extracellular side of rhodopsin is up and the cytoplasmic side is down (cf. text). Adapted with permission from Ref. [24].

axis was established, relative to the local membrane frame, by theoretically simulating the ^{2}H NMR line shape as a function of the tilt angle θ between the average membrane normal $\mathbf{n_0}$ and the main magnetic field $\mathbf{B_0}$ (tilt series). For the dark state, ^{2}H NMR spectra are shown in Fig. 2a acquired at $T=-150$ °C for aligned rhodopsin/POPC (1:50) membranes, with retinal ^{2}H-labeled at the C5-, C9-, or C13-methyl groups, respectively. The spectra in Fig. 2a were acquired at the $\theta=0°$ orientation of the membrane normal with respect to the magnetic field $\mathbf{B_0}$, where the line shape is the most sensitive to the methyl group orientation θ_B. Similar studies were conducted at temperatures of $T=-60$ and -30 °C. The ^{2}H NMR spectra exhibit little temperature dependence over a broad range of 120 °C. Theoretical simulations are superimposed on the experimental ^{2}H NMR data. In this way, values of the C–C^{2}H$_3$ bond orientations of $70°\pm3°$, $52°\pm3°$, and $68°\pm2°$ were determined for the C5-, C9-, and C13-methyl groups of retinal in the dark state of rhodopsin. The data are interpreted in terms of average bond orientations and average torsion angles of the retinylidene ligand. Accurate bond orientations of the ^{2}H-labeled methyl groups were obtained, despite the appreciable mosaic spread ($\sigma=18°$–$21°$). Values for the mosaic spread are larger than in previous studies of aligned purple membranes containing bR [50]. This may be due to the fact that rhodopsin ($M_r=40$ kDa) is a larger molecule than bR ($M_r=26$ kDa), with substantial extramembranous domains [137]. These values differ significantly from previously published work [74,136]; however, they are in good agreement with independent results from X-ray crystallography [2,4].

For analysis of the retinal conformation, a simple model with three planes of unsaturation was applied (Fig. 2), encompassing the β-ionone ring and the polyene chain to either side of the C12–C13 bond [52,59,63,133,138]. Relative orientations of pairs of ^{2}H-labeled methyl substituents are used to calculate effective dihedral angles for the planes of unsaturation. The ^{2}H NMR data for aligned samples allow one to determine the orientation of the retinal ligand within the binding cavity of rhodopsin. Each plane (designated A, B, or C) is defined by two vectors and needs two angular constraints (degrees of freedom) to specify its spatial orientation. The three molecular planes have two bonds in common, so that a total of four independent parameters (degrees of freedom) is needed to define the retinal structure. Since data for the C1*R,S* methyl groups are unavailable, the electronic transition dipole moment of the retinylidene chromophore from linear dichroism measurements was introduced as a fourth orientational restraint [126,139–141]. The values of the torsion angles $\chi_{i,k}$ between the A, B, and C planes are given by [52]

$$\chi_{i,k} = \cos^{-1}\left(\frac{\cos\theta_i\cos\theta_B^{(i,k)} - \cos\theta_B^{(i)}}{\sin\theta_i\sin\theta_B^{(i,k)}}\right) - \cos^{-1}\left(\frac{\cos\theta_k\cos\theta_B^{(i,k)} - \cos\theta_B^{(k)}}{\sin\theta_k\sin\theta_B^{(i,k)}}\right) \quad (9)$$

In the above formula, $\theta_B^{(i)}$ and $\theta_B^{(k)}$ are the orientations of the individual methyl groups attached to consecutive planes to the local membrane normal $\mathbf{n}$, and θ_i and θ_k are angles of the two methyl axes to the C_i–C_k bond with torsion angle $\chi_{i,k}$, such as the C6–C7 or the C12–C13 bond. The C_i–C_k bond angle to the local membrane normal is $\theta_B^{(i,k)}$ and is calculated from the C9-methyl orientation, together with the transition dipole moment. Multiple solutions for the torsion angles between the A, B, or C planes (and multiple retinal geometries) are obtained which correspond to a single set of experimental methyl bond orientations. For retinal, a total of 64 combinations for the relative orientations of the A, B, and C planes are possible, yielding 128 possible retinal configurations. Circular dichroism (CD) data [138,142] and carbon–carbon distances obtained from solid-state rotational-resonance ^{13}C NMR studies [22,73] can then be introduced to find a single physical solution in analogy with solution NMR spectroscopy.

Using Eq. (9), one obtains for the angle between planes B and C that $\chi_{9,13}=+150°\pm4°$ ($+147°\pm4°$) (Fig. 2b). The two values correspond to a C11═C12–C13 bond angle of 120° or 130° accordingly. The distortion of the C11═C12–C13 bond angle from ideal orbital geometry may occur due to the interaction of the C13-methyl group with the retinal hydrogen H10 or may be induced by the specific configuration of the rhodopsin binding pocket. For the β-ionone ring, using positional restraints for the C8-to-C18 and C8-to-C16/C17 distances from ^{13}C NMR [22] together with the chirality from CD studies [142], the physical solution for the C6–C7 dihedral angle is $\chi_{5,9}=-65°\pm6°$. It constitutes a negatively twisted 6-*s*-*cis* conformation as illustrated in Fig. 2b. To further establish the 11-*cis*-retinylidene structure derived from ^{2}H NMR, it was inserted into the binding pocket of the X-ray structure of rhodopsin in the dark state with the highest available resolution (2.2 Å; PDB accession code 1U19) [4]. The Schiff base end was superimposed with the nitrogen of Lys^{296}, thus keeping the carbon atoms from C12 to C15 near the X-ray coordinates. Nevertheless, a simple three-plane model does not fit into the binding pocket due to multiple steric clashes of retinal with the side chains of Tyr^{178} and Cys^{187} in extracellular loop E2 as well as Met^{207}, Tyr^{268}, and Ala^{292} in helices H5, H6, and H7, respectively. The only way to resolve this difficulty was by assuming an additional twist of the C11═C12 bond of the polyene chain [24]. In the extended three-plane model, the C11═C12 dihedral angle was determined by fitting the C10-to-C20 and C11-to-C20 distances to ^{13}C NMR rotational-resonance data [73]. It was found that the C11═C12 torsion angle is $-25°\pm10°$ and the C12–C13 torsion angle is $176°\pm6°$, where the twist is predominantly localized to the C11═C12 bond. The C10-to-C20 and C11-to-C20 distances are relatively insensitive to the C11═C12 torsion angle, giving somewhat large errors. The corresponding structure for retinal is shown in Fig. 2c, where the rhodopsin N-terminus is at top (extracellular side) and the C-terminus is at bottom (cytoplasmic side).

In this way, structural studies of the retinal chromophore by ^{2}H NMR spectroscopy reveal twisting of the retinal molecule in the dark state, which is in agreement with other biophysical studies [2,22,52,63,66,67,75,76,128,138,141,143–146], and is key to understanding its photoreaction dynamics [47,147–149]. Of particular significance for rhodopsin is the torsional twisting around the C11═C12 double bond, together with the β-ionone ring [63]. The nonplanar structure of the retinal ligand is also indicated by the presence of HOOP modes in resonance Raman [47,148,150,151] and FTIR [66] spectroscopy, and by CD studies [67,138,143,145]. All of these aspects are pertinent to explaining how the photonic energy is released and used in the triggering of visual signaling by rhodopsin in photoreceptor membranes [67,75,76,138,145].

4.2. Structural changes of retinal upon photoisomerization involve steric clashes that trigger rhodopsin activation

Next, the meta I state was cryotrapped in planar-supported bilayers to investigate changes in the retinal conformation and orientation induced by light absorption. Fig. 3a–c display ^{2}H NMR spectra acquired at -100 °C for macroscopically aligned POPC membranes at $\theta=0°$ tilt angle. Comparing the meta I state to the dark state, the largest differences in the ^{2}H NMR spectra were found for the C9–C^{2}H$_3$ group, with smaller variations for the C5–C^{2}H$_3$ and C13–C^{2}H$_3$ groups. These differences manifest the bond orientation θ_B as well as the mosaic spread σ. In the meta I state, orientations were determined for the C5-, C9-, and C13-methyl groups θ_B of $72°\pm4°$, $53°\pm3°$, and $59°\pm3°$, respectively. Due to the larger mosaic spread of meta I ($\sigma=22°$–$25°$) compared to the dark state ($\sigma=18°$–$21°$), the ^{2}H NMR spectra for the C9-methyl differ, whereas the bond

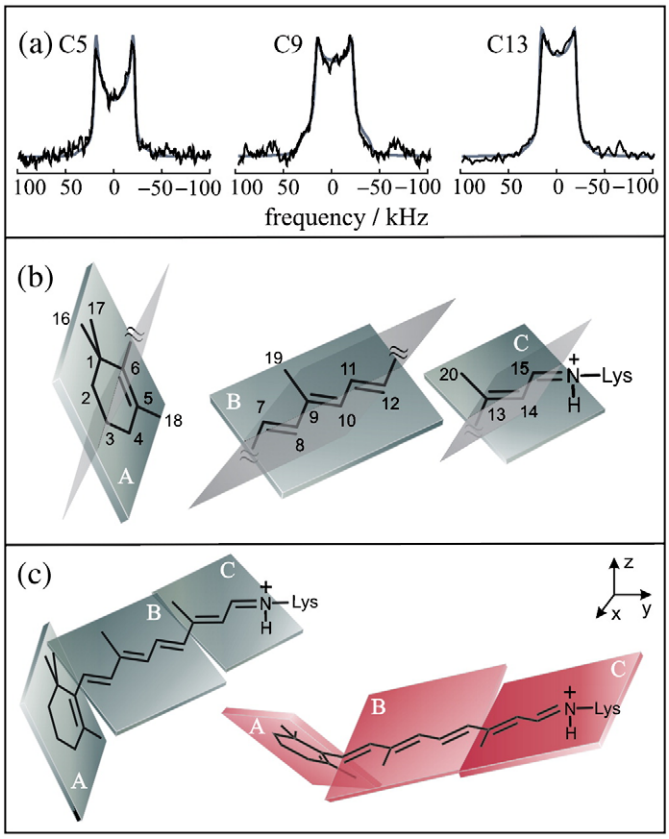

Fig. 3. Retinal structure in meta I is established by ^{2}H NMR spectroscopy. Three planes of unsaturation (A, B, C) are assumed. (a) Simulations of solid-state ^{2}H NMR spectra provide orientations of the methyl groups relative to membrane normal. Spectra are indicated for $\theta = 0°$ orientation of the average membrane normal to the static magnetic field $\mathbf{B}_0$. (b) Orientations of methyl groups and electronic transition dipole moment define orientations of the molecular fragments; two possible solutions for the planes are indicated in each case. (c) Different ^{2}H NMR structures for retinylidene ligand are eliminated using rotational-resonance ^{13}C NMR carbon–carbon distances [71,73] and molecular simulations (cf. text). Figure reprinted with permission from Ref. [53].

orientations are similar. By contrast, for the C13-methyl group a smaller spectral difference is evident despite the larger change in bond orientation. As for the dark state, the ^{2}H NMR spectra indicate that the retinylidene methyl substituents undergo rapid rotation, with order parameters for off-axial fluctuations of ≈0.9 within the meta I binding cavity.

Applying Eq. (9) and using experimental ^{13}C NMR rotational-resonance data [73] for the C10-to-C20 and C11-to-C20 carbon distances, it was found the torsion angle between the B and C planes is $\chi_{9,13} = \pm 173° \pm 4°$, which indicates an almost fully relaxed 11-*trans* conformation in the meta I state [73,152]. Possible solutions for the β-ionone ring were $\chi_{5,9} = \pm 32°$ and $\pm 57°$. The calculated meta I structures were further restrained by inserting them into the dark state rhodopsin structure [4]. It was assumed that the shape of the retinal binding cavity was nearly the same in meta I as in the dark state. Most of the retinal structures were eliminated on account of the different position of the β-ionone ring in the binding pocket, except the structure shown in Fig. 3c on the left with $\chi_{5/9} = -32°$, and $\chi_{9/13} = 173°$, and the structure obtained from it by reflection (mirror symmetry transformation) in a vertical plane with $\chi_{5/9} = 32°$, and $\chi_{9/13} = -173°$. The first structure fits best within the binding cavity, having its only close contact with the side chain of Trp^{265}. On the other hand, the mirror structure makes close contacts with the side chains of Glu^{122}, Trp^{265}, Tyr^{268}, and Ala^{292}, and therefore it is deemed less likely.

4.3. Light-induced conformational changes of retinal provide insight into activation mechanism of rhodopsin

A central question in visual signal transduction is the mechanism by which retinal is converted sequentially by light from an inverse agonist to an agonist that activates rhodopsin. The meta I and meta II states of rhodopsin correspond to the low-affinity and high-affinity forms of ligand-activated GPCRs [153]. Control of reaction selectivity through substituents of the retinal ligand and the protein environment is of significant current interest. The 11-*cis* to *trans* isomerization gives a selective relaxation of the polyene chain, whereas the β-ionone ring maintains its conformational distortion. As remarked above, the conformational strain is evident by HOOP modes in resonance Raman and FTIR spectroscopy [66,148]. Following 11-*cis* to *trans* isomerization, a gradual reduction in HOOP mode intensity of the retinylidene chromophore is seen in the various rhodopsin photointermediates [66,150,154]. A similar progressive decrease is evident in the visible CD of the rhodopsin intermediates [143], which agrees with the ^{2}H NMR analysis.

For the dark state of rhodopsin, dihedral twisting of the polyene chain entails a concerted deformation involving mainly the three consecutive bonds from the C10 to C13 carbons [47,67,73,148,152]. The torsional twisting arises from the binding cavity, which restrains the β-ionone ring within its hydrophobic pocket at one end of the molecule, and the Schiff base adjacent to its counterion at the opposite end. Steric hindrance between the C13-methyl group and hydrogen H10 of the polyene chain may also influence the torsional deformation. From the relative methyl orientations, the polyene chain has a twisted 12-*s*-*trans* conformation, which manifests the stereochemical requirements of the binding site. By contrast, a twisted 12-*s*-*cis* conformation is seen in the crystal structure of 11-*cis*-retinal [155]. For the β-ionone ring, the angular restraints from ^{2}H NMR, together with ^{13}C NMR rotational-resonance distances [22] and CD studies [138], imply that it has a negatively twisted 6-*s*-*cis* conformation, on average, in agreement with solid-state ^{13}C NMR chemical shift data [129]. The distorted 6-*s*-*cis* conformation of retinal in rhodopsin [52,59,128] and isorhodopsin [129] is distinct from the planar 6-*s*-*trans* conformation found in bacteriorhodopsin [50,156]. Hence, the protein environment can modulate the β-ionone ring conformation substantially. The negative twist about the C6–C7 bond involves non-bonded interactions between the C5-methyl of the β-ionone ring and the H8 hydrogen of the polyene chain [63,138]. However, the β-ionone ring may undergo torsional fluctuations about the C6–C7 bond and may be less restricted than the polyene chain, which is consistent with molecular dynamics simulations [57]. Mobility of the β-ionone ring within its hydrophobic binding pocket might explain the fact that it is more difficult to establish a unique conformation for this group [2,22,52,57,74,157].

Now let us consider the β-ionone ring, which may undergo a repositioning in conjunction with helical movements leading to rhodopsin activation [30,38,62,63,65,157,158]. According to ^{2}H NMR, in meta I the β-ionone ring maintains a strained conformation, which is formally 6-*s*-*cis* and is similar to the dark state [52]. Based on CD and bioorganic studies of locked retinoids, Nakanishi and coworkers [138,142] have shown that the helicity about the 6-*s*-*cis* bond is negative in the dark state and persists up to activation of the G protein, viz. the meta II state. Combined with these data, ^{2}H NMR shows that the β-ionone ring remains negatively twisted from the dark state up to meta I, in contrast to the largely relaxed *trans* polyene chain. Moreover, solid-state ^{13}C NMR chemical shift data indicate that the β-ionone ring is 6-*s*-*cis* in both rhodopsin and isorhodopsin [129], and it is proposed that it remains 6-*s*-*cis* in meta I [71] and meta II [130]. Application of a three-plane model implies that the C6–C7 torsion angle changes on average from −65° in the dark state to −32° in meta I. The difference is most likely due to a change in interaction between the β-ionone ring and the contiguous amino acid residues, arising from its displacement

toward helices H3 and H5 as further discussed below. We conclude that the average conformation about the 6-*s* bond is retained up to meta I in the steps leading to activation of rhodopsin.

Next, Fig. 4 shows the structure of retinal obtained in this work inserted into the binding pocket of the rhodopsin X-ray structure [4]. In Fig. 4a, we compare the NMR structure of retinal deduced with the extended three-plane model to the crystallographic structure [4] in the dark state. The retinylidene nitrogen atoms of the two structures are superimposed, which places the C12 to C15 atoms close to the crystallographic positions, and restrains the Schiff base end of the ligand. Relatively good agreement of the two structures is found within the uncertainties of the two methods. Dihedral twisting of the polyene stems from localization of the β-ionone ring within its hydrophobic pocket at one end of the chromophore, together with the salt bridge of the retinylidene Schiff base at the other end. The distance from the C13-methyl to the closest carbon atom of the Trp^{265} indole ring is ≈4 Å, suggesting that interactions of retinal with

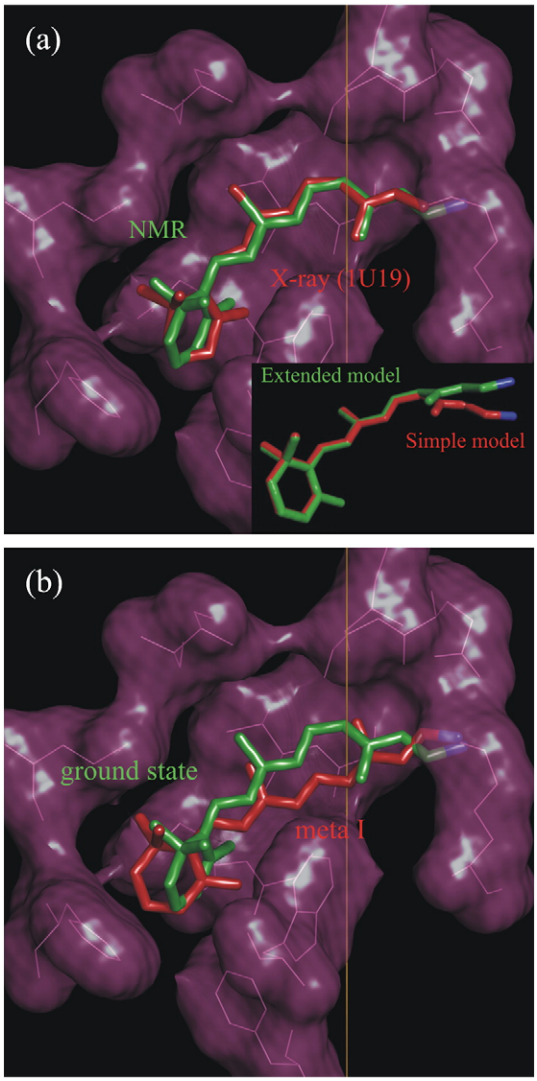

Fig. 4. Analysis of solid-state ^2H NMR data gives structure of retinal cofactor in the dark and meta I states of rhodopsin. Membrane normal corresponds to vertical direction; note that the extracellular side is up and cytoplasmic side is down. (a) NMR structure (green) of 11-*cis*-retinal in the dark state compared to retinal structure (red) from X-ray crystallography (PDB accession code 1U19) [4]. Inset: NMR structure calculated with polyene dihedral twisting about C12–C13 bond only (simple three-plane model; red) compared to structure with dihedral twisting about both the C11═C12 and C12–C13 bonds (extended three-plane model; green). (b) NMR structure for 11-*cis*-retinal in the rhodopsin dark state (green) versus NMR structure of *trans*-retinal in the meta I state (red). Figure produced with PyMOL [174]. Adapted with permission from Ref. [24].

Trp^{265} help stabilize the dark state conformation [65]. In addition, the configuration of the $-C=NH^+$- bond of the protonated Schiff base is *anti* and its hydrogen points oppositely from the C13-methyl, i.e., toward the extracellular side in the direction of the counterion Glu^{113}.

The inset to Fig. 4a displays the retinal NMR structure in the dark state as obtained with the extended three-plane model (green) compared to the NMR structure calculated using the simple three-plane model (red) [52]. The simple model leads to steric hindrance of retinal with the side chains of several amino acid residues in the binding site (Tyr^{178} and Cys^{187} in E2; Met^{207} in H5; Tyr^{268} in H6; and Ala^{292} in H7). A negative twist of the C11═C12 double bond is required to avoid these steric clashes and maintains the position of the β-ionone ring in a cavity formed by the surrounding amino acids. Dihedral twisting about the single bonds does not suffice to avoid the steric clash, due to the different geometry compared to the double bonds. Twisting about either the C9═C10 double bond or the C13═C14 bond is analogous geometrically to twisting about the C11═C12 bond; however, the distance of the Schiff base N atom from the rotation axis is less than for the C11═C12 bond and would require a greater torsional deformation. As a result, we conclude that twisting about the C11═C12 bond is energetically optimal to position the β-ionone ring within its hydrophobic cavity, while maintaining the retinylidene Schiff base near its counterion as in the dark state rhodopsin structure [4]. An interesting aspect is that pre-twisting about the 11-*cis* double bond can govern the chromophore movements upon photoexcitation, and thereby affect the ultrafast reaction dynamics. More specifically, we can propose that the binding pocket induces distortion—it prepares the retinal for the isomerization. A negative direction of isomerization about the C11═C12 bond is consistent with hybrid quantum mechanics/molecular mechanics simulations, which indicate that steric interaction of the C13-methyl with Ala^{117} hinders rotation toward positive angles [75]. The positive helical twist about the C12–C13 bond is in agreement with CD and bioorganic studies of locked retinoids [138] and with our previous results [52]. Similar conclusions regarding in-plane bonding and local twisting involving the C11═C12 and C12–C13 bonds have been reached from combined quantum mechanics/molecular mechanics simulations [58,76].

In Fig. 4b, we show the NMR structure proposed for retinal in the meta I state (red), as compared to the NMR structure of retinal in the dark state of rhodopsin (green). The retinal structure for meta I is inserted into the dark state rhodopsin binding cavity, which is justified by the similar electron densities of meta I and the dark state at low to medium resolution [159]. The Schiff base nitrogen atoms of both structures were aligned as a further positional constraint. As can be seen, the *trans* polyene chain is essentially relaxed and is nearly planar [53,152] while maintaining a significant twisting of the β-ionone ring. Moreover, the Schiff base end of the retinylidene chromophore is rotated about the polyene chain axis versus the rest of the molecule. Assuming a three-plane model, the Schiff base hydrogen would switch from facing the extracellular side in the dark state to the cytoplasmic side in meta I. This may have implications for a (possibly complex) counterion switch and deprotonation of the Schiff base, as discussed elsewhere [32,33,151].

One can also establish from Fig. 4b that a small displacement (about 1 Å) occurs of the β-ionone ring toward helix H5 and a steric clash of the retinal polyene chain with Trp^{265}. In addition, the β-ionone ring is noticeably turned toward Glu^{122} on helix H3. A simple reason for these changes is the retinal straightening due to 11-*cis* to *trans* isomerization. We should emphasize that ^2H NMR spectroscopy can determine the structure and orientation of the retinal but not its position in the binding pocket. Consequently, the picture presented in Fig. 4b is approximate with respect to the retinal location. Apparently, due to the steric clash between Trp^{265} and the retinal, these groups must move away from each other. The β-ionone ring moves toward

Glu[122], whereas Trp[265] is displaced toward helix H5 and the cytoplasmic side of the membrane. These motions play a pivotal role in the activation process. The β-ionone ring is responsible for disruption of the hydrogen-bonding network around Glu[122], which connects helices H3 and H5, and stabilizes the inactive rhodopsin conformation [31], whereas Trp[265] displacement underlies the outward rotation of the helix H6 [23,25,65,130]. We shall return to those points later in conjunction with the retinal dynamics and activation mechanism.

5. Solid-state ^{2}H NMR relaxation allows experimental investigations of molecular dynamics of retinal chromophore

As a next step, we show that NMR relaxation of the retinylidene methyl groups provides a unique, site-directed probe of the local dynamics within the ligand-binding pocket. A brief summary of the current findings is the following. (*i*) Three distinct methyl environments are found in the dark state, where the crucial C9-methyl group has the greatest mobility within the rhodopsin binding pocket; the C13-methyl is intermediate in its mobility; and the C5-methyl group of the β-ionone ring has the slowest motion. (*ii*) These site-specific differences are linked to the activation mechanism of rhodopsin. In meta I and meta II, a partial relaxation of the ligand occurs which results in two environments, one for the polyene chain, and the other for the β-ionone ring. The differences in mobility represent non-bonded interactions that occur in conjunction with formation of the activated meta II state. (*iii*) Changes in the methyl group dynamics upon photoisomerization are explained by an activation mechanism whereby retinal stays in nearly the same environment, and does not experience significant reorientation or displacement upon transition from meta I to the activated meta II state. Light-induced isomerization of retinal yields a small displacement of the ligand, causing disruption of the hydrogen-bonding network due to interaction of the β-ionone ring with Glu[122] and resulting in activating helical movements. These findings may also have implications for the activation mechanisms of other class A GPCRs.

5.1. Retinal dynamics within the rhodopsin binding cavity are probed by ^{2}H NMR relaxation time measurements

Deuterium spin-lattice (Zeeman) relaxation time (T_{1Z}) studies employed either non-aligned (powder-type) samples or aligned samples on ultrathin glass slides. ^{2}H spin-lattice relaxation times were determined for the C5-, C9-, and C13-methyl groups of retinal for rhodopsin in the dark state, with an 11-*cis*-retinylidene chromophore, as well as the meta I and meta II states having an all-*trans* retinal ligand within the binding pocket. In the dark state, measurements were conducted with both non-oriented (powder-type) samples as well as oriented samples as a function of temperature over a wide range from −160° to −30°. Use of samples aligned between ultrathin glass slides with relatively low optical density allowed trapping and characterization of the meta I and meta II states of rhodopsin using UV/visible spectroscopy. Membranes of different lipid composition were used to shift the equilibrium from the meta I to meta II state [36,37] or vice versa to stabilize the desired rhodopsin photointermediate. By conducting measurements below the freezing point of water, the interfering signal from the residual ^{2}H nuclei of the water was eliminated. The ^{2}H NMR studies were conducted below the melting temperature of the POPC lipid bilayer (−4 °C), whereby rotational diffusion of the rhodopsin molecules within the membrane was suppressed, to reveal the internal dynamics of the receptor-bound ligand.

Inversion-recovery ^{2}H NMR spectra for rhodopsin containing retinal labeled specifically at the C5-, C9-, or C13-methyl groups in aligned POPC membranes (1:50 molar ratio) in the dark state show that the rate of spin-lattice relaxation differs by as much as an order of magnitude or more for different methyl groups, depending on the temperature. Since the RQCs derived from the solid-state ^{2}H NMR spectra are essentially the same, the relaxation differences must be due to the rates of methyl spinning rather than the amplitude of the off-axial motions. Site-specific significant differences exist in the internal mobility of the retinal ligand in the dark state. For the dark state, the ^{2}H NMR relaxation results [160] indicate a monotonic temperature dependence for the T_{1Z} relaxation times of the C9- and C13-methyl groups, where T_{1Z} increases with the temperature. By contrast, a T_{1Z} curve with a minimum at −120 °C is observed for the C5-methyl group. The observation of a T_{1Z} minimum is important because it corresponds to an optimal matching of the spectral density of the thermal molecular fluctuations to the nuclear Larmor frequency ω_0. It follows that $\tau_c \approx 1/\omega_0$, which enables an effective correlation time τ_c for the motion to be obtained at the corresponding temperature in accord with NMR relaxation theory. The different T_{1Z} minima allow essentially model-free conclusions to be reached about the mobility of the retinylidene methyl groups within the binding pocket of rhodopsin in terms of differences in correlation times. Shifting the minimum to lower temperature corresponds to faster motions and vice versa. For the C9- and C13-methyl groups, all motional correlation times are less than $1/\omega_0 \approx 13$ ns down to −160 °C, whereas for the C5-methyl group, the experimental rotational correlation time exceeded 13 ns at temperatures below approximately −100 °C.

5.2. NMR relaxation theory connects experimental measurements to molecular fluctuations of biomembrane components

Further consideration of the rotational dynamics (e.g., discrete jumps, continuous diffusion) of the retinylidene methyl groups gives detailed information about the ligand fluctuations within the rhodopsin binding pocket (Fig. 5). The spin-lattice relaxation rates are related to the spectral density (power spectrum) of the thermal

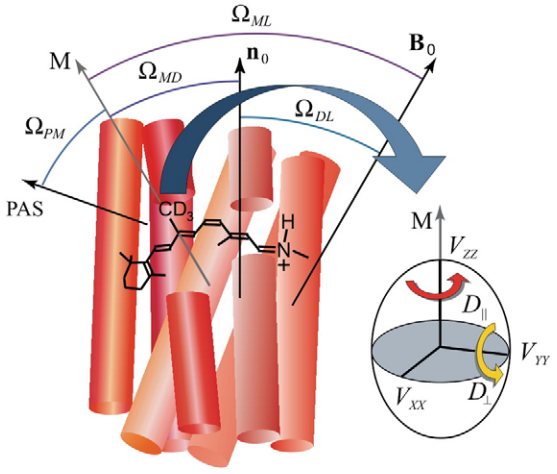

Fig. 5. Solid-state ^{2}H NMR relaxation of retinal cofactor within rhodopsin binding pocket manifests steric hindrance of spinning methyl groups. Rotational dynamics of methyl groups of retinal are formulated either as axial three-fold jumps (rate constant k) or alternatively diffusion within a potential of mean torque (diffusion coefficients $D_{\parallel}$ and $D_{\perp}$ for axial and off-axial rotations). Note that the correlation times for three-fold jumps and continuous axial diffusion have the same activation energy; only the pre-exponential factors differ. Retinal geometry is characterized by Euler angles Ω_{PM} for transformation of principal axis system (PAS) of the C–^{2}H bond (electric field gradient) to the methyl rotor axis (M); Ω_{MD} for rotation of methyl axis to membrane normal $\mathbf{n_0}$ (director, D); Ω_{ML} for rotation of methyl axis to laboratory frame (L); and lastly Ω_{DL} for rotation of the membrane normal to the laboratory frame defined by the external magnetic field $\mathbf{B_0}$.

fluctuations of the quadrupolar coupling tensor near the resonance frequency according to [161]

$$R_{1Z} = 1/T_{1Z} = \frac{3}{4}\pi^2\chi_Q^2[J_1(\omega_0) + 4J_2(2\omega_0)] \quad (10)$$

and

$$R_{1Q} = 1/T_{1Q} = \frac{9}{4}\pi^2\chi_Q^2 J_1(\omega_0) \quad (11)$$

where χ_Q is the static quadrupolar coupling constant and ω_0 is the resonance (Larmor) frequency. In these formulas, $J_m(m\omega_0)$ denotes the spectral densities ($m=1,2$) for aligned samples:

$$J_m(\omega) = \sum_{r,q} |D_{0r}^{(2)}(\Omega_{PI})|^2 \left[\langle |D_{rq}^{(2)}(\Omega_{IM})|^2\rangle - |\langle D_{rq}^{(2)}(\Omega_{IM})\rangle|^2\delta_{r0}\delta_{q0}\right] j_{rq}^{(2)}(\omega)|D_{qm}^{(2)}(\Omega_{ML})|^2 \quad (12)$$

The quantities in square brackets are the mean-squared amplitudes of the fluctuations. Assuming exponential relaxation, the corresponding reduced spectral densities of the fluctuations are given by

$$j_{rq}^{(2)}(\omega) = 2\tau_{rq}/\left(1+\omega^2\tau_{rq}{}^2\right) \quad (13)$$

Referring to Fig. 5, $D_{nm}^{(2)}(\Omega_{ij})$ are the Wigner rotation matrix elements and $\Omega_{ij} \equiv (\alpha_{ij}, \beta_{ij}, \gamma_{ij})$ are the Euler angles describing the relative orientation of the coordinate systems i and j, where $i,j = P,I,M,D,L$. In addition, P denotes the principal axis system of the electric field gradient tensor for a deuterium atom (principal axis parallel to the C–^{2}H bond), I specifies the coordinate system related to the instantaneous orientation of the labeled methyl group, M indicates the system characterizing the average methyl group orientation, and L signifies the laboratory system (external magnetic field). According to this notation for the retinylidene methyl groups, $\Omega_{PI} = (0, 70.5°, 0)$ and $\Omega_{ML} = (0, \beta_{ML}, 0)$. If the tilt of the sample (the angle between the average membrane normal and magnetic field) is $\theta = 0°$, then β_{DL} corresponds to the orientation of the methyl rotor axis relative to the membrane normal. The final coordinate transformation can be further expanded to include the dependence on the membrane orientation relative to the main magnetic field $\mathbf{B_0}$:

$$D_{qm}^{(2)}(\Omega_{ML}) = \sum_n D_{qn}^{(2)}(\Omega_{MD})D_{nm}^{(2)}(\Omega_{DL}) \quad (14)$$

For unoriented (powder-type) samples, averaging over all membrane tilt angles is performed [161].

Now the choice of a specific motional model enters into the correlation times which appear in the reduced spectral densities, Eq. (13). In general, NMR relaxation is relatively insensitive to the form of the potential, although differences between jump and continuous diffusion models have been observed for methyl groups in solid amino acids [162]. In this work, the relaxation was observed to be exponential within experimental error for all temperatures employed [163]. Since deviations from exponential relaxation are not observed, one can adopt the azimuthal average for an N-site jump model [164]. Alternatively, a continuous diffusion model may be employed explicitly [161]. If rotation about a single axis is considered, i.e., off-axial motion is neglected as in the case of a methyl group, then the above results simplify to [165]

$$J_m(\omega) = \sum_{r\neq 0} |D_{0r}^{(2)}(\Omega_{PI})|^2 j_r^{(2)}(\omega)|D_{rm}^{(2)}(\Omega_{IL})|^2 \quad (15)$$

where [161,164]

$$1/\tau_{rq} \rightarrow 1/\tau_r = \begin{cases} 4k\sin^2(\pi r/N) & (N\text{-site jump with azimuthal averaging}) \\ r^2 D_\parallel & (\text{axial diffusion}) \end{cases} \quad (16)$$

Here k is the rate constant for N-fold axial nearest neighbor jumps and $D_\parallel$ is the axial rotational diffusion constant.

The results can also be generalized to consider both axial and off-axial motions. For simplicity, a model of continuous rotational diffusion in a potential of mean torque [161] is adopted in this work [166]. The rotational correlation times are then:

$$\frac{1}{\tau_{rq}} = \frac{\mu_{rq}}{\langle |D_{rq}^{(2)}(\Omega_{IM})|^2\rangle - |\langle D_{rq}^{(2)}(\Omega_{IM})\rangle|^2\delta_{r0}\delta_{q0}} D_\perp + (D_\parallel - D_\perp)r^2 \quad (17)$$

where $D_\parallel$ and $D_\perp$ are the diffusion coefficients for rotation of the labeled methyl group about its three-fold axis and the off-axial fluctuations, correspondingly. In addition, μ_{qn} and $\langle |D_{qn}^{(2)}(\Omega_{MD})|^2\rangle$ are the moments and mean-squared moduli of the Wigner rotation matrix elements for a generalized potential of mean torque [105,166]. Their values are tabulated in terms of the order parameters in Ref. [166]. In the limit of a strong collision approximation, the methyl orientation is assumed to change randomly by any amount due to rapid variations in the torque acting upon the segment. The orientation after a collision is independent of that before a collision, and the time taken for a transition is negligible. Hence, the orientation after a collision is given by the orientational probability distribution leading to [161]

$$1/\tau_{rq} \rightarrow 1/\tau_r = 6D_\perp + (D_\parallel - D_\perp)r^2 \quad (18)$$

Finally, if it is assumed that the correlation times follow an Arrhenius activation law, then the temperature dependence for either the N-site jump [164] or continuous diffusion [161] model is a simple exponential. For the $N=3$-site jump model $1/\tau_{rq} \rightarrow 1/\tau_r = 3k$ where

$$k = k_0 \exp(-E_a/RT) \quad (19)$$

Here k_0 is the jump rate in the absence of the potential and E_a is the potential barrier height or activation energy. For a continuous rotational diffusion model, $1/\tau_r$ is related to the principal values of the rotational diffusion tensor, Eq. (18), such that

$$D_\parallel = D_{0\parallel}\exp(-E_{a\parallel}/RT) \quad (20)$$

and

$$D_\perp = D_{0\perp}\exp(-E_{a\perp}/RT) \quad (21)$$

The pre-exponential factors ($D_{0||}$, $D_{0\perp}$) correspond to the maximum diffusion constants when $E_a \ll RT$, i.e., at infinite temperature. The values of k_0 (or D_0) and E_a describe the local protein packing influences on retinal within the rhodopsin binding pocket.

5.3. ^{2}H NMR relaxation shows site-specific variations in molecular dynamics of retinal chromophore in the dark state of rhodopsin

Both the three-fold jump model of axial methyl rotations [164] and the continuous diffusion model [161] were applied to fit the T_{1Z} temperature dependences [163]. In principle, T_{1Z} measurements at different orientations for aligned samples or at different frequencies for the powder-type samples allow one to distinguish between the different possible motional formalisms. The axial jump model predicts a 20% difference in the methyl relaxation depending on orientation, whereas for an axial free diffusion model the methyl relaxation is angle independent [164]. For powder-type samples, due to the relatively low signal-to-noise ratio, T_{1Z} was measured for the $\theta = 90°$ orientation of the methyl axis to the main magnetic field $\mathbf{B_0}$, whereas the aligned samples were studied at $\theta = 0°$. Differences in the relaxation times for different orientations were undetectable

within the error of the measurements, consistent with a diffusion model for the methyl rotational dynamics. Because the predicted relaxation anisotropy for a jump model is comparable with the 10% error of the T_{1Z} measurements, a firm conclusion cannot be reached in this regard. For the diffusion model, the $\eta_D = D_{||}/D_{\perp}$ ratio could not be determined unambiguously, which was assumed to be either $\eta_D = 1$ or ∞ (axial diffusion). Correlation times are found in the range of 2–12 ps at 30° and 3–45 ps at −60 °C, depending on the methyl position, which are in the range expected for methyl rotation.

Values of the pre-exponential factors k_0 as well as the activation energies E_a from the relaxation analysis are summarized graphically in Fig. 6. For the dark state, for either model the largest values of k_0 (or D_0 for continuous diffusion) and E_a are obtained for the C5-methyl group, and the smallest values of k_0 and E_a for the C9-methyl group, with the results for the C13-methyl falling in-between. (For the rotational diffusion model, variations in E_a do not exceed 20% depending on whether only axial diffusion ($D_{\perp} = 0$) is considered or off-axial motions ($D_{\perp} = D_{||}$) are also considered.) One can immediately say that in the dark state, the mobilities of the C5-, C9-, and C13-methyl groups are all distinct; there are three different methyl environments. At any given temperature, the different correlation times for the methyl groups are due to differences in the pre-exponential factors (corresponding to motion within the potential well) and the activation energies (corresponding to the barrier height) (Fig. 6).

Because the order parameters are approximately the same for the methyl groups of retinal, the angular amplitude of the fluctuations of the methyl rotor axes must be similar. Thus, if only ^{2}H NMR spectra were recorded of powder-type samples, one would conclude that there are few differences among the various retinylidene methyl groups. Surprisingly, however, the ^{2}H NMR relaxation studies show that there are site-specific variations in the dynamics, as manifested by both the pre-exponential factor and activation barriers for the retinal motions (Fig. 6). Site-specific variations in the methyl barriers

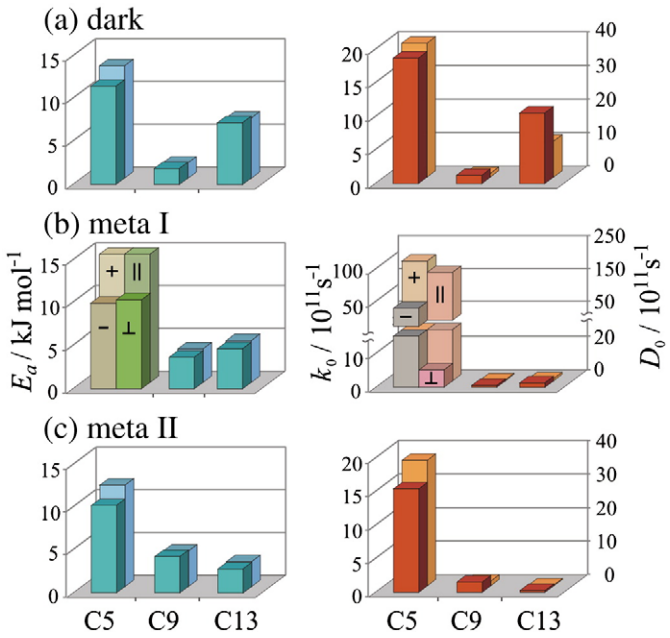

Fig. 6. Analysis of NMR relaxation data reveals site-specific dynamics of retinal underlying the rhodopsin activation mechanism. (a–c) Summary of results for the dark, meta I, and meta II states respectively. Methyl rotation is treated as axial three-fold jumps (with rate constant k) or alternatively continuous diffusion (with coefficients $D_{||}$ and $D_{\perp}$). The pre-exponential factor is either k_0 for three-fold axial jumps or D_0 for continuous diffusion, and E_a is the barrier height (activation energy). For the diffusion model, results are included for $D_{\perp} = 0$ (in the front) and $\eta_D = D_{||}/D_{\perp} = 1$ (in the back) except for the C5-methyl of the β-ionone ring in meta I, where both axial (||) and off-axial (⊥) motions are included with $\eta_D \neq 1$ or alternatively a two-conformer model with both positive (+) and negative (−) C5═C6–C7═C8 dihedral angles and $D_{\perp} = 0$.

in a protein have been seen also in the SH3 domain from α-spectrin [167]. Activation energies correspond to the temperature dependence of the relaxation rates and derived correlation times and assume an Arrhenius activation law (vide supra). Values of the experimentally determined activation energies range from 2 to 15 kJ/mol, depending on the methyl position, and are essentially independent of whether a three-fold jump or continuous diffusion model is considered. The highest activation energy is for the C5-methyl with $E_a \approx 15$ kJ/mol and is typical of methyl groups in organic solids. This value indicates either steric hindrance within the retinal or strong interactions with the protein binding pocket. The lower E_a for the C13-methyl group reflects moderate interactions within the retinal H10 hydrogen and most likely Trp^{265}. The very low E_a for the C9-methyl shows few interactions with the binding pocket, and even intra-retinal interactions seem to be compensated.

It is also noteworthy that the activation energies for retinal within the highly constrained rhodopsin binding pocket (Fig. 6) are substantially less than typically found in quantum mechanical calculations of rotational barriers. It is well established that the barriers for three-fold methyl rotation are often about 12 kJ/mol (3 kcal/mol) in organic compounds. However, for the C9- and C13-methyl groups, the activation barrier for methyl rotation from ^{2}H NMR relaxation are much lower. It is reassuring that a typical value of $E_a = 10$–15 kJ/mol is obtained for the C5-methyl group of the β-ionone ring, which is validation that our approach yields expected methyl group values [168,169]. But how does one explain the presence of a smaller barrier than expected, e.g., as in the case of the C9-methyl group? One could argue that the differences are due to the choice of dynamical models. While the correlation times and order parameters are not model-free quantities, this is less so for the barrier heights. The barrier heights assume only an Arrhenius law and are relatively independent of the choice of a motional model, e.g., three-fold jumps or continuous axial diffusion. A possible explanation for the dynamics of the C9-methyl group is that they are primarily governed by intramolecular C9-to-H7 and C9-to-H11 (1,6) interactions, which can be approximated by three-fold rotational potentials. The methyl rotameric potentials are in anti-phase, i.e., they are shifted relative to one another by about 180°, thus producing a shallow resultant potential. This idea is further supported by an effective reduction of the activation energy of the C13-methyl group in the meta I and meta II states (Fig. 6), where (1,6) interactions occur for C13- similar to the C9-methyl since the retinal is now all-*trans* with respect to the dark state.

On the other hand, the dynamics of the C5-methyl of the β-ionone ring and the C13-methyl group adjacent to the PSB may be affected in principle by intra-retinal (1,7) interactions with the H8 and H10 hydrogens, respectively. However, it is more likely that they are determined by non-bonded interactions with surrounding amino acids in the binding pocket. The 2.2 Å resolution X-ray structure [4] indicates that Glu^{122} is in close proximity to the C5-methyl group, and Trp^{265} and Tyr^{268} are close to the C13-methyl. According to the ^{2}H NMR structure, Fig. 4a, a high rotational barrier for the C5-methyl group is the result of its interaction with Glu^{122}, which is in agreement with an FTIR study of desmethyl analogs of retinal bound to rhodopsin [31]. Interestingly, ^{2}H NMR relaxation implies that the C5-methyl is the least mobile, despite that the β-ionone ring may have multiple conformations that interconvert within the hydrophobic binding pocket on a longer time scale [57].

5.4. Changes in molecular dynamics of retinal after isomerization are evident in the meta I and meta II states

An important finding of this work is that upon light activation there are only two distinct methyl environments due to relaxation of the strain of the retinal chromophore. Significant differences in the relaxation behavior for the C5- and C9-methyl groups are evident in the meta I and meta II states compared to the dark state. The largest

light-induced change involves the C9-methyl group, which is known to be crucial to the process of rhodopsin activation [46]. The E_a for the C9-methyl group is markedly increased (approximately by a factor of two). At the same time, the E_a value for the C13-methyl group is reduced in the meta I state and the values of T_{1Z} for the C9- and C13-methyl groups become nearly the same. This seems logical because following the 11-*cis* to all-*trans* isomerization, the C13- and C9-methyl groups are now on the same side of the molecule, and they experience a similar intra-retinal potential. The reduction of the C13-methyl activation energy in meta I can be explained as in the case of the C9-methyl group in the dark state by anti-phase potentials for the intra-retinal C13-to-H11 and C13-to-H15 (1,6) interactions. The more restricted mobility for the C9-methyl upon isomerization may be related to a more crowded environment, e.g., due to a smaller C9-to-H11 distance in all-*trans* retinal with respect to 11-*cis*-retinal, or non-bonded interactions with Tyr^{268} as a result of the C9-methyl rotation toward the tyrosine phenyl ring in the course of isomerization. By contrast, differences remain between the C5-methyl group of the β-ionone ring and the two other methyl groups. For the C5-methyl group in meta I, noticeable changes are observed in the temperature dependence of the T_{1Z} relaxation times (Fig. 6). Fitting of the experimental relaxation data requires two components with different activation energies E_a and pre-exponential factors (k_0 and D_0). The two components may correspond to rotation of the methyl groups and reorientation of the β-ionone ring, or alternatively two 6-*s*-*cis* conformers of the retinal with positive and negative torsion angles for the C6–C7 bond may be present [57].

Another interesting finding is that few changes are observed in the dynamics of the retinal upon the transition from the meta I to the meta II state. In Fig. 6, the activation energy E_a and diffusion constant D_0 increase slightly for the C9-methyl group and decrease for the C13-methyl. The meta II state is of particular interest because it is the activated receptor conformation [170]. In meta II, the mobility of the C9- and C13-methyl groups is similar, but with some minor differences. This is because the all-*trans* retinal in the meta II state is relaxed, which means that intra-retinal potentials for the C9- and C13-methyl groups should be close. Some of the differences in the rotational dynamics and the activation energies of the C9- and C13-methyl groups in meta II most likely can be attributed to interactions with amino acid side chains forming the chromophore binding pocket. The higher E_a for the C9-methyl group is probably the result of its interaction with Tyr^{268}, yet the relatively low activation energy of the C9-methyl in the meta II state indicates the absence of steric clashes of this group with the binding pocket. This implies that the roll angle of the central part of the retinal polyene chain, which includes the C9-methyl, does not change appreciably after isomerization. The roll angle of the retinal is mainly determined by positioning the C9-methyl between Thr^{118} and Tyr^{268}. Consequently, the part of the chain including the C13-methyl adopts an orientation similar to the C9-methyl. This is consistent with the structure of retinal in the meta I state obtained by ^{2}H NMR spectroscopy [24]. Surprisingly, the C13-methyl group has an even lower activation energy E_a for axial rotation than the C9-methyl, although with such an orientation it should be very close to the β4 strand on extracellular loop E2. A possible explanation for the absence of interactions between the C13-methyl and Cys^{187} on β4 is a displacement of the retinal polyene chain and the E2 loop away from each other, which is in agreement with ^{13}C NMR distance measurements [26]. According to our relaxation data, such a displacement already takes place in the meta I state. Interestingly, the overall behavior of the T_{1Z} relaxation times for the C5-methyl group in the dark, meta I, and meta II states is quite similar (the differences in E_a hardly exceed 20% for a given model of the rotational dynamics, see Fig. 6). Apparently, in all three states the C5-methyl group and the β-ionone ring stay in almost the same environment involving the H3/H5 helical interface. A similar conclusion has been reached based on ^{13}C NMR chemical shift data [23].

6. Relaxation of retinylidene methyl groups gives important clues to triggering of the activation process of rhodopsin

What are the changes in the ligand-binding pocket that occur upon light activation? Solid-state ^{2}H NMR spectroscopy enables one to further address the following questions. (*i*) What is the role of methyl groups in rhodopsin activation? (*ii*) Which parts of the retinal move with respect to the protein (corresponding to the work done by the ligand on the protein)? (*iii*) Does the work done by retinal on the protein involve motion of the part that is proximal or distal to the C11═C12 double bond, or both? (*iv*) Which domains of the protein move with respect to the lipid bilayer (corresponding to the work done by the protein on the membrane)? In this regard, studies of acyclic retinoids [31,59,157] show that the β-ionone ring is crucial to visual excitation and signaling. In the dark state, the β-ionone ring occupies a hydrophobic pocket consisting of residues Glu^{122}, Met^{207}, Phe^{208}, His^{211}, Phe^{212}, and Trp^{265}. The C5-methyl group is located between Glu^{122} and Trp^{265}. Recent FTIR [31] and X-ray studies [6] suggested that the β-ionone ring is implicated in the disruption of a hydrogen-bonding network around Glu^{122}, which stabilizes the inactive rhodopsin conformation. At the opposite end of the retinal cofactor, 11-*cis* to *trans* isomerization about the C11═C12 double bond changes the pK_a of the protonated Schiff base, destabilizing its interactions with the Glu^{113} counterion. A counterion switch in meta I [33] and eventually deprotonation in the meta II state [34] leads to breaking of the ionic lock involving the protonated Schiff base and its carboxylate counterion. Now according to ^{2}H NMR, there are three different types of methyl behavior in the dark state, which is rather striking support for the idea that the retinylidene cofactor has three different interaction sites [138]. The reduction from three environments to two environments upon 11-*cis* to *trans* isomerization could be due to a diminution of the conformational strain within the rhodopsin binding pocket [53]. Moreover, as mentioned above, neither the C9- nor C13-methyl mobility has changed appreciably upon the transition from the meta I to meta II state. The dynamics of the C5-methyl of the β-ionone ring remains largely the same in all three states. This finding suggests that the major structural relaxation involving the retinal cofactor occurs already at the meta I intermediate in the activation process, and that the β-ionone ring is not expelled from its hydrophobic pocket in the molecular mechanism that gives rise to the activated receptor.

According to the ^{2}H NMR structure proposed for retinal in the pre-activated meta I state [24,53], the major changes upon isomerization involve reorientation of the C13-methyl group together with the Schiff base end of the ligand, which give rise to a switch of the electrostatic interactions with the salt bridge involving the (potentially complex) counterion [34]. On the other hand, the β-ionone ring and the polyene with its C9-methyl group occupy similar binding sites in meta I as in the dark state. This is supported by the structure of meta I obtained from electron crystallography, where the β-ionone ring maintains its position up to the meta I state [159], as well as ^{13}C chemical shift data [23]. By contrast, significant motion of the β-ionone ring following light activation is suggested by the results of cross-linking experiments [62], which would mean that expulsion of the β-ionone ring from its pocket occurs at the meta II state, potentially triggering interactions with helix H4 in the receptor activation mechanism. In addition, translational motion of retinal relative to the protein is supported by the results of dipolar-assisted rotational-resonance (DARR) studies [25], involving a 4–5 Å (1.5–2 Å in later work [130]) displacement of the retinal toward helix H5. This would mean that interactions of the β-ionone ring with the binding pocket would be altered significantly. The latest DARR distance measurements in the meta II state [26] and opsin crystal structures [39,40] reveal extracellular loop E2 motion accompanied by rearrangement of hydrogen-bonding interactions around E2, which are believed to be involved in rhodopsin activation. This is also supported

by our relaxation data. Further disruption of a second ionic lock involving the E(D)RY motif in H3 [34] exposes key receptor binding sites for the G protein (transducin) coupling.

The following sequence of events in the activation process emerges from comparison of the ^{2}H NMR relaxation data in the dark, meta I, and meta II states with FTIR results [31], the solid-state ^{13}C NMR distance measurements in the meta II state [26,130], and the opsin X-ray structures [39,40]. The latter structures are assumed to resemble the active rhodopsin conformation. We suggest that in the early photointermediates (batho and lumi) the retinal ligand is highly distorted due to torsional twisting and bending away from the ideal sp^2 hybrid orbital geometry of the polyene [6,171]. Induced fit of the retinal chromophore in the dark state is no longer possible within the rhodopsin binding pocket upon photoisomerization [24]. As shown in Fig. 7a and b, steric clash of the C13-methyl with the extracellular E2 loop results in the rearrangement of hydrogen-bonding networks connecting E2 with the extracellular ends of transmembrane helices H4, H5, and H6. As a consequence, movement of E2 and the retinal away from each other together with the straightening of the ligand leads to a steric clash of its polyene chain with Trp^{265} (Fig. 7). This is confirmed by the reduced distance between the C9-methyl and Trp^{265} in the meta II state [65]. The steric clash with Trp^{265} and straightening of the polyene chain result in the displacement of the β-ionone ring toward Glu^{122} on helix H3, yielding a disruption of the hydrogen-bonding network around Glu^{122}. The group on the β-ionone ring that most likely interacts with Glu^{122} is the C5-methyl group. This explains its much higher activation energy for axial spinning compared to the C9- and C13-methyl groups, especially in meta I (Fig. 6). Displacement of the β-ionone ring toward helix H3 is supported by the recent X-ray

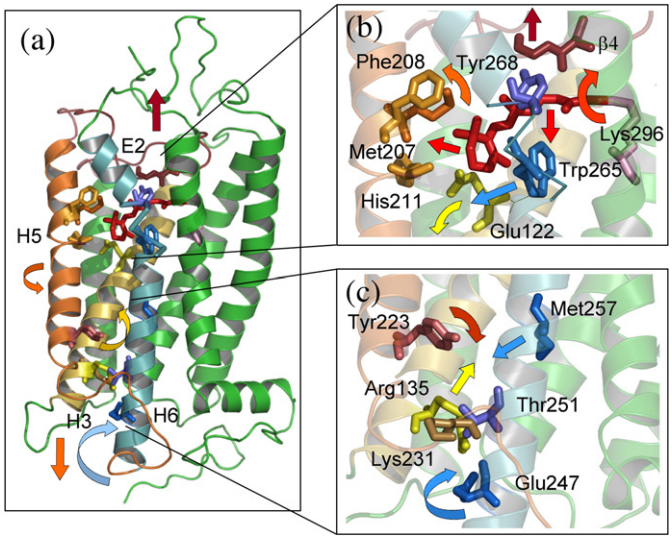

Fig. 7. Mechanism of rhodopsin activation involves conformational changes in the binding pocket and cytoplasmic side of the protein following chromophore photoisomerization. (a) Concerted rearrangement of the extracellular E2 loop and helices H5, H6, and H3. (b) Due to geometry of the binding pocket and the ligand pre-twisting around the C11═C12 bond in the dark state, retinal isomerization occurs in the direction indicated. The C9-methyl group prevents rotation of the chromophore about its long axis; hence, the C13-methyl group rotates upwards toward the β4 strand of the extracellular loop E2. The C13-methyl pushes E2 and the retinal polyene chain away from each other. Concomitantly, the retinal β-ionone ring moves toward Glu^{122} and Met^{207} due to the retinal straightening, together with the steric hindrance between the polyene chain and Trp^{265}. Disruption of the hydrogen-bonding networks around Glu^{122} and the E2 loop as well as the ionic lock between the protonated Schiff base and counterions Glu^{181} and/or Glu^{113} (see text) destabilizes the inactive rhodopsin conformation. (c) Rearrangements of helices H5 and H6 in the cytoplasmic region [39] renders a second ionic lock involving Glu^{134}, Arg^{135}, and Glu^{247} in the inactive rhodopsin state [26] less favorable than Arg^{135}–Tyr^{223} and Glu^{247}–Lys^{231} interactions. The latter are assumed to be maintained in the activated meta II conformation [26,40]. The activation mechanism is highly cooperative suggesting that large-scale conformational fluctuations of the protein at lower frequencies are involved.

structure of lumirhodopsin [6], where movement of the β-ionone ring away from Trp^{265} is observed, together with distortion and outward motion of the middle of H3 encompassing Gly^{120}, Gly^{121}, and Thr^{118}.

Straightening of the retinal polyene chain and separation of the β-ionone ring from Trp^{265} are evident in earlier MD simulations [171] and constitutes a major change in rhodopsin structure after photoisomerization. The energy initially stored in the distorted retinal is transformed into non-bonding interactions of retinal with its environment, followed by increased mobilities of some parts of the protein including kinked regions of the helices, mainly helix H6 [171]. Movement of the retinal β-ionone ring away from Trp^{265} creates the necessary free volume for Trp^{265} to move closer to helix H5. The retinal polyene chain pushes Trp^{265} toward H5 and the cytoplasmic side of the protein (shown by an arrow in Fig. 7). Such a displacement of Trp^{265} is believed to be responsible for the outward rotation of the cytoplasmic side of the helix H6 [23,25], which is considered to be a key change in rhodopsin conformation involved in receptor activation and G protein binding [41,172]. Another recently discovered change in the opsin [39] structure compared to rhodopsin is the elongation of helix H5 and movement of its cytoplasmic end closer to H6. The H5 helix rearrangement is coupled to the displacement of the E2 loop away from the retinal [26]. This helical movement apparently brings Tyr^{223} on H5 closer to Arg^{135} on H3 and leads to the disruption of the ionic lock formed by Glu^{134} and Arg^{135} on H3 and Glu^{247} on H6. Formation of a new hydrogen-bonding network involving Arg^{135}, Tyr^{223}, Glu^{247}, and Lys^{231} stabilizes the active rhodopsin conformation as in opsin [39].

Clearly, the conformational changes of rhodopsin are intricately interconnected; although the motions are concerted they do not take place simultaneously. For example, deprotonation of the Schiff base does not occur until the meta II state is reached [32], whereas the ^{2}H NMR relaxation data suggest that the β4 strand displacement happens already in the meta I state. On the other hand, breaking of the ionic lock involving Glu^{134}, Arg^{135}, and Glu^{247} takes place in the meta I to meta II transition [34]. This agrees with the slightly higher activation energy for axial rotation of the C5-methyl group in the meta I state (15 kJ/mol versus about 12 kJ/mol in the dark and meta II states). The absence of appreciable changes in the C5-methyl dynamics from the dark to the meta I and meta II states can be explained by a corresponding displacement of the surrounding Glu^{122} and Trp^{265} side chains. Similar considerations can be applied to Met^{207} and His^{211}, which are near to the β-ionone ring. This would explain the absence of ^{13}C NMR chemical shift changes for carbons C16 and C17 in the activated state [23]. It has also been suggested that helix H5 rotates counterclockwise (looking at rhodopsin from the extracellular side) [26] to break the second ionic lock (cf. Fig. 7c). We find this hypothesis plausible, although the opsin structure does not show any appreciable rotation of H5. One may certainly argue, however, that it is absent in the opsin apoprotein on account of the lack of retinal. The possibility for helical rotations due to low potential barriers has been shown recently by a computational study [173]. Apart from the energy stored in highly distorted retinal after isomerization, additional contributions from low-frequency conformational fluctuations of the protein may be needed to overcome potential barriers to reach the active conformation, as in the case of protein folding [29]. The H5 rotation can be explained as a result of displacement of the β-ionone ring away from Trp^{265} toward helices H3 and H5, accompanied by steric interactions with Met^{207} and His^{211}. Hypothetically, a steric clash between the C5-methyl group of the β-ionone ring and Glu^{122} may lead to the clockwise rotation of helix H3, which would move Arg^{135} closer to Tyr^{223} and facilitate disruption of the second ionic lock to form the active meta II state. Such putative helical rotations could preserve the local environment of the β-ionone ring and the C5-methyl group dynamics in particular.

Lastly, within the framework of the suggested activation mechanism (Fig. 7), one can explain the functional significance of the

retinylidene methyl groups and the reduced activity of rhodopsin when regenerated with desmethyl retinals. For example, the C5-methyl group is responsible for the interaction with Glu^{122}, and its deletion leads to the less effective disruption of the hydrogen-bonding network connecting helices H3 and H5. Deletion of the C13-methyl has a similar effect on displacement of the E2 loop and rearrangement of the surrounding hydrogen bonds. The C9-methyl deletion could lead to reorientation of the retinal polyene chain toward Tyr^{268} and reduce or eliminate the steric clash of the C13-methyl with the extracellular E2 loop, having the same effect. It may also cause repositioning of the β-ionone ring and influence its interactions with Glu^{122} [35]. All these methyl deletions prevent one or a few conformational changes required for the meta II formation, and they backshift the metarhodopsin equilibrium toward the inactive meta I state.

7. Conclusions

Solid-state NMR constitutes a powerful avenue for investigation of protein dynamics that is complementary to the other biophysical approaches such as X-ray crystallography. Using ^2H NMR the structure and dynamics of 11-*cis*-retinal in the rhodopsin dark state have been compared with all-*trans* retinal in the meta I and meta II photointermediates. In the dark state, the cofactor is a highly potent inverse agonist, yet retinal is transformed to an agonist in meta II. Despite its phenomenal dark state stability retinal has significant dynamics within the binding pocket of rhodopsin. The ^2H NMR data indicate that the methyl groups are rapidly spinning but that the off-axial motions are highly restricted, with order parameters of $S_{C_3} \approx 0.9$. In consequence, the NMR relaxation rates are determined mainly by fast axial methyl rotation about their three-fold axes. An activation mechanism is suggested whereby the β-ionone ring remains within its hydrophobic pocket, and the environment of the C5-methyl group of the β-ionone ring is largely preserved in the activated meta II state versus either the meta I or dark states. Disruption of hydrogen-bonding networks stabilizing the inactive conformation occurs due to a steric clash of the ligand C13-methyl group with the β4 strand of the second extracellular loop, together with displacement of the β-ionone ring toward Glu^{122} on helix H3. According to this proposal, cooperative motion of the ligand, E2 loop, and helices H5 and H6 is accompanied by additional conformational changes within the protein that yield exposure of recognition sites for transducin on the cytoplasmic domain of rhodopsin, resulting in visual perception.

Acknowledgments

Research was supported in part by grants from the US NIH (EY012049 and EY018891). We thank K. Tanaka, S. Krane, and K. Nakanishi for generously providing isotopically labeled retinal and C. Job for conducting preliminary experiments. Discussions with K. P. Hofmann, W. L. Hubbell, J. W. Lewis, and R. Vogel are gratefully acknowledged.

References

[1] K. Palczewski, T. Kumasaka, T. Hori, C.A. Behnke, H. Motoshima, B.A. Fox, I. Le Trong, D.C. Teller, T. Okada, R.E. Stenkamp, M. Yamamoto, M. Miyano, Crystal structure of rhodopsin: a G protein-coupled receptor, Science 289 (2000) 739–745.
[2] D.C. Teller, T. Okada, C.A. Behnke, K. Palczewski, R.E. Stenkamp, Advances in determination of a high-resolution three-dimensional structure of rhodopsin, a model of G-protein-coupled receptors (GPCRs), Biochemistry 40 (2001) 7761–7772.
[3] T. Okada, Y. Fujiyoshi, M. Silow, J. Navarro, E.M. Landau, Y. Shichida, Functional role of internal water molecules in rhodopsin revealed by x-ray crystallography, Proc. Natl. Acad. Sci. U.S.A. 99 (2002) 5982–5987.
[4] T. Okada, M. Sugihara, A.-N. Bondar, M. Elstner, P. Entel, V. Buss, The retinal conformation and its environment in rhodopsin in light of a new 2.2 Å crystal structure, J. Mol. Biol. 342 (2004) 571–583.
[5] J. Li, P.C. Edwards, M. Burghammer, C. Villa, G.F.X. Schertler, Structure of bovine rhodopsin in a trigonal crystal form, J. Mol. Biol. 343 (2004) 1409–1438.
[6] H. Nakamichi, T. Okada, Local peptide movement in the photoreaction intermediate of rhodopsin, Proc. Natl. Acad. Sci. U. S. A. 103 (2006) 12729–12734.
[7] D. Salom, D.T. Lodowski, R.E. Stenkamp, I. Le Trong, M. Golczak, B. Jastrzebska, T. Harris, J.A. Ballesteros, K. Palczewski, Crystal structure of a photoactivated deprotonated intermediate of rhodopsin, Proc. Natl. Acad. Sci. U.S.A. 103 (2006) 16123–16128.
[8] V. Cherezov, D.M. Rosenbaum, M.A. Hanson, S.G.F. Rasmussen, F.S. Thian, T.S. Kobilka, H.-J. Choi, P. Kuhn, W.I. Weis, B.K. Kobilka, R.C. Stevens, High-resolution crystal structure of an engineered human β_2-adrenergic G protein-coupled receptor, Science 318 (2007) 1258–1265.
[9] S.G.F. Rasmussen, H.J. Choi, D.M. Rosenbaum, T.S. Kobilka, F.S. Thian, P.C. Edwards, M. Burghammer, V.R.P. Ratnala, R. Sanishvili, R.F. Fischetti, G.F.X. Schertler, W.I. Weis, B.K. Kobilka, Crystal structure of the human β_2 adrenergic G-protein-coupled receptor, Nature 450 (2007) 383–387.
[10] D.M. Rosenbaum, V. Cherezov, M.A. Hanson, S.G.F. Rasmussen, F.S. Thian, T.S. Kobilka, H.J. Choi, X.J. Yao, W.I. Weis, R.C. Stevens, B.K. Kobilka, GPCR engineering yields high-resolution structural insights into β_2-adrenergic receptor function, Science 318 (2007) 1266–1273.
[11] B. Kobilka, G.F.X. Schertler, New G-protein-coupled receptor crystal structures: insights and limitations, Trends Pharmacol. Sci. 29 (2008) 79–83.
[12] T. Warne, M.J. Serrano-Vega, J.G. Baker, R. Moukhametzianov, P.C. Edwards, R. Henderson, A.G.W. Leslie, C.G. Tate, G.F.X. Schertler, Structure of a β_1-adrenergic G-protein-coupled receptor, Nature 454 (2008) 486–491.
[13] C. Toyoshima, M. Nakasako, H. Nomura, H. Ogawa, Crystal structure of the calcium pump of sarcoplasmic reticulum at 2.6 Å resolution, Nature 405 (2000) 647–655.
[14] J. Abramson, I. Smirnova, V. Kasho, G. Verner, H.R. Kaback, S. Iwata, Structure and mechanism of the lactose permease of *Escherichia coli*, Science 301 (2003) 610–615.
[15] C. Fernandez, K. Adeishvili, K. Wuthrich, Transverse relaxation-optimized NMR spectroscopy with the outer membrane protein OmpX in dihexanoyl phosphatidylcholine micelles, Proc. Natl. Acad. Sci. U. S. A. 98 (2001) 2358–2363.
[16] P.M. Hwang, W.Y. Choy, E.I. Lo, L. Chen, J.D. Forman-Kay, C.R.H. Raetz, G.G. Privé, R.E. Bishop, L.E. Kay, Solution structure and dynamics of the outer membrane enzyme PagP by NMR, Proc. Natl. Acad. Sci. U.S.A. 99 (2002) 13560–13565.
[17] T.S. Ulmer, A. Bax, N.B. Cole, R.L. Nussbaum, Structure and dynamics of micelle-bound human α-synuclein, J. Biol. Chem. 280 (2005) 9595–9603.
[18] A. Lange, K. Giller, S. Hornig, M.-F. Martin-Eauclaire, O. Pongs, S. Becker, M. Baldus, Toxin-induced conformational changes in a potassium channel revealed by solid-state NMR, Nature 440 (2006) 959–962.
[19] U.H.N. Durr, L. Waskell, A. Ramamoorthy, The cytochromes P450 and b_5 and their reductases—promising targets for structural studies by advanced solid-state NMR spectroscopy, Biochim. Biophys. Acta 1768 (2007) 3235–3259.
[20] M. Etzkorn, S. Martell, O.C. Andronesi, K. Seidel, M. Engelhard, M. Baldus, Secondary structure, dynamics, and topology of a seven-helix receptor in native membranes, studied by solid-state NMR spectroscopy, Angew. Chem., Int. Ed. 46 (2007) 459–462.
[21] A. Watts, Solid-state NMR in drug design and discovery for membrane-embedded targets, Nat. Rev. Drug Disc. 4 (2005) 555–568.
[22] P.J.R. Spooner, J.M. Sharples, M.A. Verhoeven, J. Lugtenberg, C. Glaubitz, A. Watts, Relative orientation between the β-ionone ring and the polyene chain for the chromophore of rhodopsin in native membranes, Biochemistry 41 (2002) 7549–7555.
[23] P.J.R. Spooner, J.M. Sharples, S.C. Goodall, P.H.M. Bovee-Geurts, M.A. Verhoeven, J. Lugtenburg, A.M.A. Pistorius, W.J. DeGrip, A. Watts, The ring of the rhodopsin chromophore in a hydrophobic activation switch within the binding pocket, J. Mol. Biol. 343 (2004) 719–730.
[24] A.V. Struts, G.F.J. Salgado, K. Tanaka, S. Krane, K. Nakanishi, M.F. Brown, Structural analysis and dynamics of retinal chromophore in dark and meta I states of rhodopsin from ^2H NMR of aligned membranes, J. Mol. Biol. 372 (2007) 50–66.
[25] A.B. Patel, E. Crocker, M. Eilers, A. Hirshfeld, M. Sheves, S.O. Smith, Coupling of retinal isomerization to the activation of rhodopsin, Proc. Natl. Acad. Sci. U.S.A. 101 (2004) 10048–10053.
[26] S. Ahuja, V. Hornak, E.C.Y. Yan, N. Syrrett, J.A. Goncalves, A. Hirshfeld, M. Ziliox, T.P. Sakmar, M. Sheves, P.J. Reeves, S.O. Smith, M. Eilers, Helix movement is coupled to displacement of the second extracellular loop in rhodopsin activation, Nat. Struct. Mol. Biol. 15 (2009) 168–175.
[27] H. Frauenfelder, P.W. Fenimore, G. Chen, B.H. McMahon, Protein folding is slaved to solvent motions, Proc. Natl. Acad. Sci. U. S. A. 103 (2006) 15469–15472.
[28] D.U. Ferreiro, J.A. Hegler, E.A. Komives, P.G. Wolynes, Localizing frustration in native proteins and protein assemblies, Proc. Natl. Acad. Sci. U. S. A. 104 (2007) 19819–19824.
[29] S.B. Ozkan, G.A. Wu, J.D. Chodera, K.A. Dill, Protein folding by zipping and assembly, Proc. Natl. Acad. Sci. U. S. A. 104 (2007) 11987–11992.
[30] W.L. Hubbell, C. Altenbach, C.M. Hubbell, H.G. Khorana, Rhodopsin structure, dynamics, and activation: a perspective from crystallography, site-directed spin labeling, sulfhydryl reactivity, and disulfide cross-linking, Adv. Prot. Chem. 63 (2003) 243–290.
[31] R. Vogel, F. Siebert, S. Lüdeke, A. Hirshfeld, M. Sheves, Agonists and partial agonists of rhodopsin: retinals with ring modifications, Biochemistry 44 (2005) 11684–11699.

[32] S. Lüdeke, R. Beck, E.C.Y. Yan, T.P. Sakmar, F. Siebert, R. Vogel, The role of Glu181 in the photoactivation of rhodopsin, J. Mol. Biol. 353 (2005) 345–356.
[33] K. Martínez-Mayorga, M.C. Pitman, A. Grossfield, S.E. Feller, M.F. Brown, Retinal counterion switch mechanism in vision evaluated by molecular simulations, J. Am. Chem. Soc. 128 (2006) 16502–16503.
[34] M. Mahalingam, K. Martínez-Mayorga, M.F. Brown, R. Vogel, Two protonation switches control rhodopsin activation in membranes, Proc. Natl. Acad. Sci. U. S. A. 105 (2008) 17795–17800.
[35] R. Vogel, S. Lüdeke, F. Siebert, T.P. Sakmar, A. Hirshfeld, M. Sheves, Agonists and partial agonists of rhodopsin: retinal polyene methylation affects receptor activation, Biochemistry 45 (2006) 1640–1652.
[36] M.F. Brown, Modulation of rhodopsin function by properties of the membrane bilayer, Chem. Phys. Lipids 73 (1994) 159–180.
[37] A.V. Botelho, T. Huber, T.P. Sakmar, M.F. Brown, Curvature and hydrophobic forces drive oligomerization and modulate activity of rhodopsin in membranes, Biophys. J. 91 (2006) 4464–4477.
[38] T.P. Sakmar, S.T. Menon, E.P. Marin, E.S. Awad, Rhodopsin: insights from recent structural studies, Annu. Rev. Biophys. Biomol. Struct. 31 (2002) 443–484.
[39] J.H. Park, P. Scheerer, K.P. Hofmann, H.-W. Choe, O.P. Ernst, Crystal structure of the ligand-free G-protein-coupled receptor opsin, Nature 454 (2008) 183–188.
[40] P. Scheerer, J.H. Park, P.W. Hildebrand, Y.J. Kim, N. Krauß, H.-W. Choe, K.P. Hofmann, O.P. Ernst, Crystal structure of opsin in its G-protein-interacting conformation, Nature 455 (2008) 497–503.
[41] D.L. Farrens, C. Altenbach, K. Yang, W.L. Hubbell, H.G. Khorana, Requirement of rigid-body motion of transmembrane helices for light activation of rhodopsin, Science 274 (1996) 768–770.
[42] B. Knierim, K.P. Hofmann, O.P. Ernst, W.L. Hubbell, Sequence of late molecular events in the activation of rhodopsin, Proc. Natl. Acad. Sci. U.S.A. 104 (2007) 20290–20295.
[43] C. Altenbach, A.K. Kusnetzow, O.P. Ernst, K.P. Hofmann, W.L. Hubbell, High-resolution distance mapping in rhodopsin reveals the pattern of helix movement due to activation, Proc. Natl. Acad. Sci. U.S.A. 105 (2008) 7439–7444.
[44] I.D. Alves, G.F.J. Salgado, Z. Salamon, M.F. Brown, G. Tollin, V.J. Hruby, Phosphatidylethanolamine enhances rhodopsin photoactivation and transducin binding in a solid supported lipid bilayer as determined using plasmon-waveguide resonance spectroscopy, Biophys. J. 88 (2005) 198–210.
[45] Z. Salamon, M.F. Brown, G. Tollin, Plasmon resonance spectroscopy: probing molecular interactions within membranes, Trends Biochem. Sci. 24 (1999) 213–219.
[46] R. Vogel, G.-B. Fan, M. Sheves, F. Siebert, The molecular origin of the inhibition of transducin activation in rhodopsin lacking the 9-methyl group of the retinal chromophore: a UV-Vis and FTIR spectroscopic study, Biochemistry 39 (2000) 8895–8908.
[47] P. Kukura, D.W. McCamant, S. Yoon, D.B. Wandschneider, R.A. Mathies, Structural observation of the primary isomerization in vision with femtosecond-stimulated Raman, Science 310 (2005) 1006–1009.
[48] J.W. Lewis, D.S. Kliger, Absorption spectroscopy in studies of visual pigments: spectral and kinetic characterization of intermediates, Meth. Enzymol. 315 (2000) 164–178.
[49] A.S. Ulrich, I. Wallat, M.P. Heyn, A. Watts, Re-orientation of retinal in the M-photointermediate of bacteriorhodopsin, Nature Struct. Biol. 2 (1995) 190–192.
[50] S. Moltke, A.A. Nevzorov, N. Sakai, I. Wallat, C. Job, K. Nakanishi, M.P. Heyn, M.F. Brown, Chromophore orientation in bacteriorhodopsin determined from the angular dependence of deuterium NMR spectra of oriented purple membranes, Biochemistry 37 (1998) 11821–11835.
[51] S.M. Moltke, I. Wallat, N. Sakai, K. Nakanishi, M.F. Brown, M.P. Heyn, The angles between the C_1-, C_5-, and C_9-methyl bonds of the retinylidene chromophore and the membrane normal increase in the M intermediate of bacteriorhodopsin: direct determination with solid-state ^{2}H NMR, Biochemistry 38 (1999) 11762–11772.
[52] G.F.J. Salgado, A.V. Struts, K. Tanaka, N. Fujioka, K. Nakanishi, M.F. Brown, Deuterium NMR structure of retinal in the ground state of rhodopsin, Biochemistry 43 (2004) 12819–12828.
[53] G.F.J. Salgado, A.V. Struts, K. Tanaka, S. Krane, K. Nakanishi, M.F. Brown, Solid-state ^{2}H NMR structure of retinal in metarhodopsin I, J. Am. Chem. Soc. 128 (2006) 11067–11071.
[54] K. Varga, L. Ashmovska, I. Parrot, M.T. Dauvergne, M. Haertlein, V. Forsyth, A. Watts, NMR crystallography: the effect of deuteration on high resolution ^{13}C solid state NMR spectra of a 7-TM protein, Biochim. Biophys. Acta 1768 (2007) 3029–3035.
[55] A.V. Botelho, N.J. Gibson, Y. Wang, R.L. Thurmond, M.F. Brown, Conformational energetics of rhodopsin modulated by nonlamellar forming lipids, Biochemistry 41 (2002) 6354–6368.
[56] M.F. Brown, K. Martínez-Mayorga, K. Nakanishi, G.F.J. Salgado, A.V. Struts, Retinal conformation and dynamics in activation of rhodopsin illuminated by solid-state ^{2}H NMR spectroscopy, Photochem. Photobiol. 85 (2009) 442–453.
[57] P.-W. Lau, A. Grossfield, S.E. Feller, M.C. Pitman, M.F. Brown, Dynamic structure of retinylidene ligand of rhodopsin probed by molecular simulations, J. Mol. Biol. 372 (2007) 906–917.
[58] S. Hayashi, E. Tajkhorshid, K. Schulten, Photochemical reaction dynamics of the primary event of vision studied by means of a hybrid molecular simulation, Biophys. J. 96 (2009) 403–416.
[59] K. Nakanishi, R. Crouch, Application of artificial pigments to structure determination and study of photoinduced transformations of retinal proteins, Isr. J. Chem. 35 (1995) 253–272.
[60] J. Hu, R.G. Griffin, J. Herzfeld, Synergy in the spectral tuning of retinal pigments: complete accounting of the opsin shift in bacteriorhodopsin, Proc. Natl. Acad. Sci. U. S. A. 91 (1994) 8880–8884.
[61] F. Jäger, S. Jäger, O. Krautle, N. Friedman, M. Sheves, K.P. Hofmann, F. Siebert, Interactions of the β-ionone ring with the protein in the visual pigment rhodopsin control the activation mechanism. An FTIR and fluorescence study on artificial vertebrate rhodopsins, Biochemistry 33 (1994) 7389–7397.
[62] B. Borhan, M.L. Souto, H. Imai, Y. Shichida, K. Nakanishi, Movement of retinal along the visual transduction path, Science 288 (2000) 2209–2212.
[63] N. Fishkin, N. Berova, K. Nakanishi, Primary events in dim light vision: a chemical and spectroscopic approach toward understanding protein/chromophore interactions in rhodopsin, Chem. Rec. 4 (2004) 120–135.
[64] F.J. Bartl, O. Fritze, E. Ritter, R. Herrmann, V. Kuksa, K. Palczewski, K.P. Hofmann, O.P. Ernst, Partial agonism in a G protein-coupled receptor. Role of the retinal ring structure in rhodopsin activation, J. Biol. Chem. 280 (2005) 34259–34267.
[65] E. Crocker, M. Eilers, S. Ahuja, V. Hornak, A. Hirshfeld, M. Sheves, S.O. Smith, Location of Trp265 in metarhodopsin II: implications for the activation mechanism of the visual receptor rhodopsin, J. Mol. Biol. 357 (2006) 163–172.
[66] F. Siebert, Application of FTIR spectroscopy to the investigation of dark structures and photoreactions of visual pigments, Isr. J. Chem. 35 (1995) 309–323.
[67] G.G. Kochendoerfer, P.J.E. Verdegem, I. van der Hoef, J. Lugtenburg, R.A. Mathies, Retinal analog study of the role of steric interactions in the excited state isomerization dynamics of rhodopsin, Biochemistry 35 (1996) 16230–16240.
[68] Q. Wang, G.G. Kochendoerfer, R.W. Schoenlein, P.J.E. Verdegem, J. Lugtenburg, R.A. Mathies, C.V. Shank, Femtosecond spectroscopy of a 13-demethylrhodopsin visual pigment analogue: the role of nonbonded interactions in the isomerization process, J. Phys. Chem. 100 (1996) 17388–17394.
[69] J. Isele, T.P. Sakmar, F. Siebert, Rhodopsin activation affects the environment of specific neighboring phospholipids: an FTIR spectroscopic study, Biophys. J. 79 (2000) 3063–3071.
[70] K. Yang, D.L. Farrens, W.L. Hubbell, H.G. Khorana, Structure and function in rhodopsin. Single cysteine substitution mutants in the cytoplasmic interhelical E/F loop region show position-specific effects in transducin activation, Biochemistry 35 (1996) 12464–12469.
[71] P.J.R. Spooner, J.M. Sharples, S.C. Goodall, H. Seedorf, M.A. Verhoeven, J. Lugtenburg, P.H.M. Bovee-Geurts, W.J. DeGrip, A. Watts, Conformational similarities in the β-ionone ring region of the rhodopsin chromophore in its ground state and after photoactivation to the metarhodopsin-I intermediate, Biochemistry 42 (2003) 13371–13378.
[72] X. Feng, P.J.E. Verdegem, Y.K. Lee, D. Sandström, M. Edén, P. Bovee-Geurts, W.J. deGrip, J. Lugtenburg, H.J.M. deGroot, M.H. Levitt, Direct determination of a molecular torsional angle in the membrane protein rhodopsin by solid-state NMR, J. Am. Chem. Soc. 119 (1997) 6853–6857.
[73] P.J.E. Verdegem, P.H.M. Bovee-Geurts, W.J. de Grip, J. Lugtenburg, H.J.M. de Groot, Retinylidene ligand structure in bovine rhodopsin, metarhodopsin-I, and 10-methylrhodopsin from internuclear distance measurements using ^{13}C-labeling and 1-D rotational resonance MAS NMR, Biochemistry 38 (1999) 11316–11324.
[74] G. Gröbner, I.J. Burnett, C. Glaubitz, G. Choi, A.J. Mason, A. Watts, Observations of light-induced structural changes of retinal within rhodopsin, Nature 405 (2000) 810–813.
[75] J.A. Gascon, V.S. Batista, QM/MM study of energy storage and molecular rearrangements due to the primary event in vision, Biophys. J. 87 (2004) 2931–2941.
[76] M. Sugihara, J. Hufen, V. Buss, Origin and consequences of steric strain in the rhodopsin binding pocket, Biochemistry 45 (2006) 801–810.
[77] M. Baldus, Biological solid-state NMR, methods and applications, J. Biomol. NMR 39 (2007) 73–86.
[78] G. Lipari, A. Szabo, Model-free approach to the interpretation of nuclear magnetic resonance relaxation in macromolecules. 1. Theory and range of validity, J. Am. Chem. Soc. 104 (1982) 4546–4559.
[79] A.G. Palmer, NMR probes of molecular dynamics: overview and comparison with other techniques, Annu. Rev. Biophys. Biomol. Struct. 30 (2001) 129–155.
[80] A.J. Wand, Dynamic activation of protein function: a view emerging from NMR spectroscopy, Nature Struct. Biol. 8 (2001) 926–931.
[81] M.F. Brown, S.I. Chan, in: D.M. Grant, R.K. Harris (Eds.), Encyclopedia of Nuclear Magnetic Resonance, Wiley, New York, 1996, pp. 871–885.
[82] M.F. Brown, A.A. Nevzorov, ^{2}H-NMR in liquid crystals and membranes, Colloids Surf. A 158 (1999) 281–298.
[83] H.I. Petrache, M.F. Brown, in: A.M. Dopico (Ed.), Methods in Molecular Biology, Humana, Totowa, 2007, pp. 341–353.
[84] N.J. Traaseth, L. Shi, R. Verardi, D.G. Mullen, G. Barany, G. Veglia, Structure and topology of monomeric phospholamban in lipid membranes determined by a hybrid solution and solid-state NMR approach, Proc. Natl. Acad. Sci. U. S. A. 106 (2009) 10165–10170.
[85] J.J. Buffy, N.J. Traaseth, A. Mascioni, P.L. Gor'kov, E.Y. Chekmenev, W.W. Brey, G. Veglia, Two-dimensional solid-state NMR reveals two topologies of sarcolipin in oriented lipid bilayers, Biochemistry 45 (2006) 10939–10946.
[86] A. Ramamoorthy, Y.F. Wei, D.K. Lee, PISEMA solid-state NMR spectroscopy, Annu. Rep. NMR Spectr. 52 (2004) 1–52.
[87] J.D. Xu, U.H.N. Durr, S.C. Im, Z.H. Gan, L. Waskell, A. Ramamoorthy, Bicelle-enabled structural studies on a membrane-associated cytochrome b_5 by solid-state MAS NMR spectroscopy, Angew. Chem., Int. Ed. 47 (2008) 7864–7867.
[88] U.H.N. Durr, K. Yamamoto, S.C. Im, L. Waskell, A. Ramamoorthy, Solid-state NMR

reveals structural and dynamical properties of a membrane-anchored electron-carrier protein, cytochrome b_5, J. Am. Chem. Soc. 129 (2007) 6670–6671.
[89] S.K. Kandasamy, D.-K. Lee, R.P.R. Nanga, J. Xu, J.S. Santos, R.G. Larson, A. Ramamoorthy, Solid-state NMR and molecular dynamics simulations reveal the oligomeric ion-channels of TM2-$GABA_A$ stabilized by intermolecular hydrogen bonding, Biochim. Biophys. Acta 1788 (2009) 686–695.
[90] O.C. Andronesi, S. Becker, K. Seidel, H. Heise, H.S. Young, M. Baldus, Determination of membrane protein structure and dynamics by magic-angle-spinning solid-state NMR spectroscopy, J. Am. Chem. Soc. 127 (2005) 12965–12974.
[91] M.F. Brown, M.P. Heyn, C. Job, S. Kim, S. Moltke, K. Nakanishi, A.A. Nevzorov, A.V. Struts, G.F.J. Salgado, I. Wallat, Solid-State ^{2}H NMR spectroscopy of retinal proteins in aligned membranes, Biochim. Biophys. Acta 1768 (2007) 2979–3000.
[92] A.A. Nevzorov, S.J. Opella, Structural fitting of PISEMA spectra of aligned proteins, J. Magn. Res. 160 (2003) 33–39.
[93] A. McDermott, T. Polenova, Solid state NMR: new tools for insight into enzyme function, Curr. Opin. Struct. Biol. 17 (2007) 617–622.
[94] M. Hiller, V.A. Higman, S. Jehle, B.-J. van Rossum, W. Kühlbrandt, H. Oschkinat, [2,3–^{13}C]-labeling of aromatic residues-getting a head start in the magic-angle-spinning NMR assignment of membrane proteins, J. Am. Chem. Soc 130 (2008) 408–409.
[95] A. Ramamoorthy, S.K. Kandasamy, D.K. Lee, S. Kidambi, R.G. Larson, Structure, topology, and tilt of cell-signaling peptides containing nuclear localization sequences in membrane bilayers determined by solid-state NMR and molecular dynamics simulation studies, Biochemistry 46 (2007) 965–975.
[96] F. Porcelli, B. Buck, D.K. Lee, K.J. Hallock, A. Ramamoorthy, G. Veglia, Structure and orientation of pardaxin determined by NMR experiments in model membranes, J. Biol. Chem. 279 (2004) 45815–45823.
[97] K.J. Hallock, D.K. Lee, A. Ramamoorthy, MSI-78, an analogue of the magainin antimicrobial peptides, disrupts lipid bilayer structure via positive curvature strain, Biophys. J. 84 (2003) 3052–3060.
[98] A. Ramamoorthy, D.K. Lee, J.S. Santos, K.A. Henzler-Wildman, Nitrogen-14 solid-state NMR spectroscopy of aligned phospholipid bilayers to probe peptide-lipid interaction and oligomerization of membrane associated peptides, J. Am. Chem. Soc. 130 (2008) 11023–11029.
[99] S.J. Opella, C. Ma, F.M. Marassi, Nuclear magnetic resonance of membrane-associated peptides and proteins, Meth. Enzymol. 339 (2001) 285–313.
[100] Z. Zheng, R. Yang, M.L. Bodner, D.P. Weliky, Conformational flexibility and strand arrangements of the membrane-associated HIV fusion peptide trimer probed by solid-state NMR spectroscopy, Biochemistry 45 (2006) 12960–12975.
[101] N. Komi, K. Okawa, Y. Tateishi, M. Shirakawa, T. Fujiwara, H. Akutsu, Structural analysis of pituitary adenylate cyclase-activating polypeptides bound to phospholipid membranes by magic angle spinning solid-state NMR, Biochim. Biophys. Acta 1768 (2007) 3001–3011.
[102] M.L. Mak-Jurkauskas, V.S. Bajaj, M.K. Hornstein, M. Belenky, R.G. Griffin, J. Herzfeld, Energy transformations early in the bacteriorhodopsin photocycle revealed by DNP-enhanced solid-state NMR, Proc. Natl. Acad. Sci. U.S.A. 105 (2008) 883–888.
[103] R. Mani, S.D. Cady, M. Tang, A.J. Waring, R.I. Lehrert, M. Hong, Membrane-dependent oligomeric structure and pore formation of β-hairpin antimicrobial peptide in lipid bilayers from solid-state NMR, Proc. Natl. Acad. Sci. U. S. A. 103 (2006) 16242–16247.
[104] T.P. Trouard, A.A. Nevzorov, T.M. Alam, C. Job, J. Zajicek, M.F. Brown, Influence of cholesterol on dynamics of dimyristoylphosphatidylcholine as studied by deuterium NMR relaxation, J. Chem. Phys. 110 (1999) 8802–8818.
[105] A.A. Nevzorov, T.P. Trouard, M.F. Brown, Lipid bilayer dynamics from simultaneous analysis of orientation and frequency dependence of deuterium spin-lattice and quadrupolar order relaxation, Phys. Rev. E 58 (1998) 2259–2281.
[106] G.V. Martinez, E.M. Dykstra, S. Lope-Piedrafita, C. Job, M.F. Brown, NMR elastometry of fluid membranes in the mesoscopic regime, Phys. Rev. E 66 (2002) 050902–1–050902–4.
[107] M.F. Brown, R.L. Thurmond, S.W. Dodd, D. Otten, K. Beyer, Composite membrane deformation on the mesoscopic length scale, Phys. Rev. E 64 (2001) 010901–1–010901–4.
[108] M.F. Brown, R.L. Thurmond, S.W. Dodd, D. Otten, K. Beyer, Elastic deformation of membrane bilayers probed by deuterium NMR relaxation, J. Am. Chem. Soc. 124 (2002) 8471–8484.
[109] A.A. Nevzorov, S. Moltke, M.F. Brown, Structure of the A-form and B-form of DNA from deuterium NMR line shape simulation, J. Am. Chem. Soc. 120 (1998) 4798–4805.
[110] A.A. Arnold, I. Marcotte, Studying natural structural protein fibers by solid-state nuclear magnetic resonance, Concepts Magn. Reson. 34A (2009) 24–47.
[111] P. Walsh, K. Simonetti, S. Sharpel, Core structure of amyloid fibrils formed by residues 106–126 of the human prion protein, Structure 17 (2009) 417–426.
[112] J.R. Brender, E.L. Lee, M.A. Cavitt, A. Gafni, D.G. Steel, A. Ramamoorthy, Amyloid fiber formation and membrane disruption are separate processes localized in two distinct regions of IAPP, the type-2-diabetes-related peptide, J. Am. Chem. Soc. 130 (2008) 6424–6429.
[113] J.R. Brender, U.H.N. Durr, D. Heyl, M.B. Budarapu, A. Ramamoorthy, Membrane fragmentation by an amyloidogenic fragment of human Islet Amyloid Polypeptide detected by solid-state NMR spectroscopy of membrane nanotubes, Biochim. Biophys. Acta 1768 (2007) 2026–2029.
[114] J.T. Nielsen, M. Bjerring, M.D. Jeppesen, R.O. Pedersen, J.M. Pedersen, K.L. Hein, T. Vosegaard, T. Skrydstrup, D.E. Otzen, N.C. Nielsen, Unique identification of supramolecular structures in amyloid fibrils by solid-state NMR spectroscopy, Angew. Chem., Int. Ed. 48 (2009) 2118–2121.
[115] C.P. Jaroniec, C.E. MacPhee, V.S. Bajaj, M.T. McMahon, C.M. Dobson, R.G. Griffin, High-resolution molecular structure of a peptide in an amyloid fibril determined by magic angle spinning NMR spectroscopy, Proc. Natl. Acad. Sci. U. S. A. 101 (2004) 711–716.
[116] R. Tycko, Solid-state NMR as a probe of amyloid fibril structure, Curr. Opin. Chem. Biol. 4 (2000) 500–506.
[117] R. Tycko, Molecular structure of amyloid fibrils: insights from solid-state NMR, Q. Rev. Biophys. 39 (2006) 1–55.
[118] A.T. Petkova, Y. Ishii, J.J. Balbach, O.N. Antzutkin, R.D. Leapman, F. Delaglio, R. Tycko, A structural model for Alzheimer's β-amyloid fibrils based on experimental constraints from solid state NMR, Proc. Natl. Acad. Sci. U. S. A. 99 (2002) 16742–16747.
[119] J. Curtis-Fisk, R.M. Spencer, D.P. Weliky, Native conformation at specific residues in recombinant inclusion body protein in whole cells determined with solid-state NMR spectroscopy, J. Am. Chem. Soc. 130 (2008) 12568–12569.
[120] D.P. Raleigh, M.H. Levitt, R.G. Griffin, Rotational resonance in solid state NMR, Chem. Phys. Lett. 146 (1988) 71–76.
[121] A. Bax, Weak alignment offers new NMR opportunities to study protein structure and dynamics, Protein Sci. 12 (2003) 1–16.
[122] M. Billeter, G. Wagner, K. Wuthrich, Solution NMR structure determination of proteins revisited, J. Biomol. NMR 42 (2008) 155–158.
[123] M.F. Brown, S. Lope-Piedrafita, G.V. Martinez, H.I. Petrache, in: G.A. Webb (Ed.), Modern Magnetic Resonance, Springer, Heidelberg, 2006, pp. 245–256.
[124] H. Frauenfelder, The Debye–Waller factor: from villain to hero in protein crystallography, Int. J. Quantum Chem. 35 (1989) 711–715.
[125] F. Fanelli, P.G. De Benedetti, Computational modeling approaches to structure-function analysis of G protein-coupled receptors, Chem. Rev. 105 (2005) 3297–3351.
[126] J.W. Lewis, C.M. Einterz, S.J. Hug, D.S. Kliger, Transition dipole orientations in the early photolysis intermediates of rhodopsin, Biophys. J. 56 (1989) 1101–1111.
[127] K. Sakurai, A. Onishi, H. Imai, O. Chisaka, Y. Ueda, J. Usukura, K. Nakatani, Y. Shichida, Physiological properties of rod photoreceptor cells in green-sensitive cone pigment knock-in mice, J. Gen. Physiol. 130 (2007) 21–40.
[128] S.O. Smith, I. Palings, V. Copié, D.P. Raleigh, J. Courtin, J.A. Pardoen, J. Lugtenberg, R.A. Mathies, R.G. Griffin, Low-temperature solid-state ^{13}C NMR studies of the retinal chromophore in rhodopsin, Biochemistry 26 (1987) 1606–1611.
[129] S.O. Smith, I. Palings, M.E. Miley, J. Courtin, H. de Groot, J. Lugtenberg, R.A. Mathies, R.G. Griffin, Solid-state NMR studies of the mechanism of the opsin shift in the visual pigment rhodopsin, Biochemistry 29 (1990) 8158–8164.
[130] S. Ahuja, E. Crocker, M. Eilers, V. Hornak, A. Hirshfeld, M. Ziliox, N. Syrrett, P.J. Reeves, H.G. Khorana, M. Sheves, S.O. Smith, Location of the retinal chromophore in the activated state of rhodopsin, J. Biol. Chem. (2009) 10190–10201.
[131] M. Eilers, P.J. Reeves, W.W. Ying, H.G. Khorana, S.O. Smith, Magic angle spinning NMR of the protonated retinylidene Schiff base nitrogen in rhodopsin: expression of ^{15}N-lysine- and ^{13}C-glycine-labeled opsin in a stable cell line, Proc. Natl. Acad. Sci. U.S.A. 96 (1999) 487–492.
[132] K. Tanaka, A.V. Struts, S. Krane, N. Fujioka, G.F.J. Salgado, K. Martínez-Mayorga, M.F. Brown, K. Nakanishi, Synthesis of CD_3-labeled 11-*cis*-retinals and applications to solid-state deuterium NMR spectroscopy of rhodopsin, Bull. Chem. Soc. Japan 80 (2007) 2177–2184.
[133] A.A. Nevzorov, S. Moltke, M.P. Heyn, M.F. Brown, Solid-state NMR line shapes of uniaxially oriented immobile systems, J. Am. Chem. Soc. 121 (1999) 7636–7643.
[134] M.F. Brown, in: K.M. Merz Jr., B. Roux (Eds.), Biological Membranes: A Molecular Perspective from Computation and Experiment, Birkhäuser, Basel, 1996, pp. 175–252.
[135] A. Kusumi, J.S. Hyde, Spin-label saturation-transfer electron spin resonance detection of transient association of rhodopsin in reconstituted membranes, Biochemistry 21 (1982) 5978–5983.
[136] G. Gröbner, G. Choi, I.J. Burnett, C. Glaubitz, P.J.E. Verdegem, J. Lugtenberg, A. Watts, Photoreceptor rhodopsin: structural and conformational study of its chromophore 11-*cis* retinal in oriented membranes by deuterium solid state NMR, FEBS Lett. 422 (1998) 201–204.
[137] T. Huber, A.V. Botelho, K. Beyer, M.F. Brown, Membrane model for the GPCR prototype rhodopsin: hydrophobic interface and dynamical structure, Biophys. J. 86 (2004) 2078–2100.
[138] Y. Fujimoto, N. Fishkin, G. Pescitelli, J. Decatur, N. Berova, K. Nakanishi, Solution and biologically relevant conformations of enantiomeric 11-*cis*-locked cyclopropyl retinals, J. Am. Chem. Soc. 124 (2002) 7294–7302.
[139] M. Chabre, J. Breton, The orientation of the chromophore of vertebrate rhodopsin in the "meta" intermediate states and the reversibility of the meta II–meta III transition, Vision Res. 19 (1979) 1005–1018.
[140] M. Michel-Villaz, C. Roche, M. Chabre, Orientational changes of the absorbing dipole of retinal upon the conversion of rhodopsin to bathorhodopsin, lumirhodopsin, and isorhodopsin, Biophys. J. 37 (1982) 603–616.
[141] S. Jäger, J.W. Lewis, T.A. Zvyaga, I. Szundi, T.P. Sakmar, D.S. Kliger, Chromophore structural changes in rhodopsin from nanoseconds to microseconds following pigment photolysis, Proc. Natl. Acad. Sci. U.S.A. 94 (1997) 8557–8562.
[142] Y. Fujimoto, J. Ishihara, S. Maki, N. Fujioka, T. Wang, T. Furuta, N. Fishkin, B. Borhan, N. Berova, K. Nakanishi, On the bioactive conformation of the rhodopsin chromophore: absolute sense of twist around the 6-*s*-*cis* bond, Chem. Eur. J. 7 (2001) 4198–4204.
[143] T. Yoshizawa, Y. Shichida, Low-temperature circular dichroism of intermediates of rhodopsin, Meth. Enzymol. 81 (1982) 634–641.
[144] Y. Imamoto, M. Sakai, Y. Katsuta, A. Wada, M. Ito, Y. Shichida, Structure around

C_6–C_7 bond of the chromophore in bathorhodopsin: low-temperature spectroscopy of 6*s*-*cis*-locked bicyclic rhodopsin analogs, Biochemistry 35 (1996) 6257–6262.
[145] F. DeLange, P.H.M. Bovee-Geurts, J. VanOostrum, M.D. Portier, P.J.E. Verdegem, J. Lugtenburg, W.J. DeGrip, An additional methyl group at the 10-position of retinal dramatically slows down the kinetics of the rhodopsin photocascade, Biochemistry 37 (1998) 1411–1420.
[146] A.F.L. Creemers, S. Kiihne, P.H.M. Bovee-Geurts, W.J. DeGrip, J. Lugtenburg, H.J.M. de Groot, ^{1}H and ^{13}C MAS NMR evidence for pronounced ligand–protein interactions involving the ionone ring of the retinylidene chromophore in rhodopsin, Proc. Natl. Acad. Sci. U.S.A 99 (2002) 9101–9106.
[147] Q. Wang, R.W. Schoenlein, L.A. Peteanu, R.A. Mathies, C.V. Shank, Vibrationally coherent photochemistry in the femtosecond primary event of vision, Science 266 (1994) 422–424.
[148] S.W. Lin, M. Groesbeek, I. van der Hoef, P. Verdegem, J. Lugtenburg, R.A. Mathies, Vibrational assignment of torsional normal modes of rhodopsin: probing excited-state isomerization dynamics along the reactive C_{11}=C_{12} torsion coordinate, J. Phys. Chem. B 102 (1998) 2787–2806.
[149] T. Andruniów, N. Ferré, M. Olivucci, Structure, initial excited-state relaxation, and energy storage of rhodopsin resolved at the multiconfigurational perturbation theory level, Proc. Natl. Acad. Sci. U. S. A. 101 (2004) 17908–17913.
[150] D. Pan, R.A. Mathies, Chromophore structure in lumirhodopsin and metarhodopsin I by time-resolved resonance Raman microchip spectroscopy, Biochemistry 40 (2001) 7929–7936.
[151] E.C.Y. Yan, M.A. Kazmi, Z. Ganim, J.-M. Hou, D. Pan, B.S.W. Chang, T.P. Sakmar, R.A. Mathies, Retinal counterion switch in the photoactivation of the G protein-coupled receptor rhodopsin, Proc. Natl. Acad. Sci. U.S.A. 100 (2003) 9262–9267.
[152] X. Feng, P.J.E. Verdegem, M. Edén, D. Sandström, Y.K. Lee, P.H.M. Bovee-Geurts, W.J. de Grip, J. Lugtenburg, H.J.M. de Groot, M.H. Levitt, Determination of a molecular torsional angle in the metarhodopsin-I photointermediate of rhodopsin by double-quantum solid-state NMR, J. Biomol. NMR 16 (2000) 1–8.
[153] K.L. Pierce, R.T. Premont, R.J. Lefkowitz, Seven-transmembrane receptors, Nat. Rev. Mol. Cell Biol. 3 (2002) 639–650.
[154] E.C.Y. Yan, Z. Ganim, M.A. Kazmi, B.S.W. Chang, T.P. Sakmar, R.A. Mathies, Resonance Raman analysis of the mechanism of energy storage and chromophore distortion in the primary visual photoproduct, Biochemistry 43 (2004) 10867–10876.
[155] R.D. Gilardi, I.L. Karle, J. Karle, Crystal and molecular structure of 11-*cis*-retinal, Acta Cryst. B28 (1972) 2605–2612.
[156] G.S. Harbison, S.O. Smith, J.A. Pardoen, J.M.L. Courtin, J. Lugtenburg, J. Herzfeld, R.A. Mathies, R.G. Griffin, Solid-state ^{13}C NMR detection of a perturbed 6-*s*-*trans* chromophore in bacteriorhodopsin, Biochemistry 24 (1985) 6955–6962.
[157] G.-F. Jang, V. Kuksa, S. Filipek, F. Bartl, E. Ritter, M.H. Gelb, K.P. Hofmann, K. Palczewski, Mechanism of rhodopsin activation as examined with ring-constrained retinal analogs and the crystal structure of the ground state protein, J. Biol. Chem. 276 (2001) 26148–26153.
[158] S.P. Sheikh, T.A. Zvyaga, O. Lichtarge, T.P. Sakmar, H.R. Bourne, Rhodopsin activation blocked by metal-ion-binding sites linking transmembrane helices C and F, Nature 383 (1996) 347–350.
[159] J.J. Ruprecht, T. Mielke, R. Vogel, C. Villa, G.F.X. Schertler, Electron crystallography reveals the structure of metarhodopsin I, EMBO J 23 (2004) 3609–3620.
[160] A.V. Struts, K. Martinez-Mayorga, G.F.J. Salgado, M.F. Brown, Dynamics of retinal studied by ^{2}H NMR relaxation sheds new light on rhodopsin activation, Biophys. J. 96 (2009) 409A.
[161] M.F. Brown, Theory of spin-lattice relaxation in lipid bilayers and biological membranes. ^{2}H and ^{14}N quadrupolar relaxation, J. Chem. Phys. 77 (1982) 1576–1599.
[162] L.S. Batchelder, C.H. Niu, D.A. Torchia, Methyl reorientation in polycrystalline amino-acids and peptides: A ^{2}H NMR spin-lattice relaxation study, J. Am. Chem. Soc. 105 (1983) 2228–2231.
[163] A.V. Struts, G.F.J. Salgado, K. Martínez-Mayorga, C. Job, K. Tanaka, S. Krane, K. Nakanishi, M.F. Brown, ^{2}H NMR relaxation and dynamics of retinal cofactor in dark, meta I, and meta II states of rhodopsin, Biophys. J. 92 (2007) 150A–151A.
[164] D.A. Torchia, A. Szabo, Spin-lattice relaxation in solids, J. Magn. Reson. 49 (1982) 107–121.
[165] A.A. Nevzorov, M.F. Brown, Dynamics of lipid bilayers from comparative analysis of ^{2}H and ^{13}C nuclear magnetic resonance relaxation data as a function of frequency and temperature, J. Chem. Phys. 107 (1997) 10288–10310.
[166] T.P. Trouard, T.M. Alam, M.F. Brown, Angular dependence of deuterium spin-lattice relaxation rates of macroscopically oriented dilaurylphosphatidylcholine in the liquid-crystalline state, J. Chem. Phys. 101 (1994) 5229–5261.
[167] Y. Xue, M.S. Pavlova, Y.E. Ryabov, B. Reif, N.R. Skrynnikov, Methyl rotation barriers in proteins from ^{2}H relaxation data. Implications for protein structure, J. Am. Chem. Soc. 129 (2007) 6827–6838.
[168] G. Widmalm, R.W. Pastor, T.E. Bull, Molecular dynamics simulation of methyl group relaxation in water, J. Chem. Phys. 94 (1991) 4097–4098.
[169] J. Bastard, J.M. Bernassau, D.K. Duc, M. Fetizon, E. Lesueur, Rotation barriers of interacting axial methyl groups, J. Phys. Chem. 90 (1986) 3936–3941.
[170] T. Okada, O.P. Ernst, K. Palczewski, K.P. Hofmann, Activation of rhodopsin: new insights from structural and biochemical studies, Trends Biochem. Sci. 26 (2001) 318–324.
[171] J. Saam, E. Tajkhorshid, S. Hayashi, K. Schulten, Molecular dynamics investigation of primary photoinduced events in the activation of rhodopsin, Biophys. J. 83 (2002) 3097–3112.
[172] B. Knierim, K.P. Hofmann, W. Gärtner, W.L. Hubbell, O.P. Ernst, Rhodopsin and 9-demethyl-retinal analog: effect of a partial agonist on displacement of transmembrane helix 6 in class A G protein-coupled receptors, J. Biol. Chem. 283 (2008) 4967–4974.
[173] S. Bhattacharya, S.E. Hall, N. Vaidehi, Agonist-induced conformational changes in bovine rhodopsin: Insight into activation of G-protein-coupled receptors, J. Mol. Biol. 382 (2008) 539–555.
[174] W.L. DeLano, The PyMOL Molecular Graphics System, http://www.pymol.org (2002).